

# Midstream Infrastructure and Environmental Externalities in Oil and Gas: Permian Basin Flaring and Methane Emissions\*

Mark Agerton<sup>†</sup>      Wesley Blundell<sup>‡</sup>      Ben Gilbert<sup>§</sup>  
Gregory B. Upton Jr.<sup>¶</sup>

November 18, 2024  
See [latest version](#)

We estimate the short-run causal effect of congestion in natural gas transmission infrastructure on upstream environmental externalities from oil and gas production in the Permian basin between 2015 and 2021. We estimate that congestion caused 34 percent of flaring and 10 percent of methane emissions, valued at \$524M and \$674M in annual climate costs. At the well level, we find that gas wells reduce output in response to congestion, while oil wells, which produce the majority of Permian gas, do not. Instead, oil wells flare excess gas. We also find evidence that wells vertically integrated with a processing plant also respond differently compared to wells that are not, suggesting market structure matters. Our results have implications for the design of methane and flaring regulations and demonstrate how, when resources are jointly produced, transportation constraints on one resource may lead to increased pollution, not reduced production.

**JEL Codes:** L1; L5; L72; Q3; Q4; Q5

**Keywords:** flaring; methane; midstream; transmission; transportation; congestion; natural gas; shale; environmental policy

---

\*This paper was previously presented at the June 2021 AERE meeting as “The Role of Market Structure in Regulating Externalities: Evidence from the U.S. Shale Boom” and the November 2021 USAEE meeting as “Quantifying the Role of Midstream Congestion and Market Structure in Permian Flaring.” Agerton’s research was supported by the USDA National Institute of Food and Agriculture, Hatch project 1020147.

We are grateful for feedback from Cody Nehiba (LSU); Tim Fitzgerald (Texas Tech); Chuck Mason (Wyoming); and seminar participants at the University of Wyoming, Boise State University, USAEE, AERE, WEAI, and IAEE.

<sup>†</sup>Department of Agricultural and Resource Economics, University of California Davis and Non-Resident Fellow at Baker Institute for Public Policy, Rice University. [mjagerton@ucdavis.edu](mailto:mjagerton@ucdavis.edu).

<sup>‡</sup>School of Economic Sciences, Washington State University. [wesley.blundell@wsu.edu](mailto:wesley.blundell@wsu.edu)

<sup>§</sup>Department of Economics and Business and Faculty Fellow at Payne Institute for Public Policy, Colorado School of Mines. [bgilbert@mines.edu](mailto:bgilbert@mines.edu)

<sup>¶</sup>Center for Energy Studies, Louisiana State University. [gupton3@lsu.edu](mailto:gupton3@lsu.edu)

# 1 Introduction

According to the International Energy Agency (IEA), flaring of natural gas during production is responsible for 10% of the greenhouse gas emissions from the oil and gas sector.<sup>1</sup> This figure is attributable in part to recent scientific work documenting that unlit and inefficient flares are also meaningful sources of methane emissions (EDF 2021; Plant et al. 2022). Methane is a more potent greenhouse gas (hereafter “GHG”) relative to CO<sub>2</sub> generated from efficient flaring.<sup>2</sup> There have been significant policy efforts to curb flaring due to its climate costs, local health costs (Blundell and Kokoza 2022; Boslett et al. 2021; Tran et al. 2024), and the foregone market value of flared gas. Globally, these efforts include the World Bank’s Zero Routine Flaring by 2030 initiative and recently proposed methane regulations in the European Union (2019/942).<sup>3</sup> For the United States, recent policies to reduce flaring and venting include restrictions on flaring in Colorado and New Mexico, the EPA’s 2024 rule to eliminate flaring, and the Bureau of Land Management’s Methane Waste Prevention Rule.<sup>4</sup>

Flaring and methane emissions from upstream oil and gas production are the product of not only decisions in the upstream, but also conditions in the midstream. The midstream encompasses local gas gathering, gas processing, and long haul transmission infrastructure. In this paper we use detailed data from Texas’ Permian Basin to estimate the short-run impact of congestion in natural gas midstream infrastructure on upstream flaring and methane emissions from 2015 through 2021. During this time, the Permian Basin was (and is currently) the largest oil producing region in the U.S., with significant quantities of associated gas production. We find that congestion was responsible for 34 percent of Permian flaring and 10 percent of Permian methane emissions with an estimated \$1.2B in annual climate costs: \$524M due to increased flaring and \$674M due to increased methane emissions.

Several stylized facts motivate attention to the midstream segment. Oil wells often produce large amounts of associated gas as a co-product, with half of Texas Permian gas production originating from oil wells since 2013 (Appendix Figure E.3).<sup>5</sup> Firms may treat the gas as a byproduct because the oil is more valuable than the gas and because it is also more costly to transport.<sup>6</sup> Unlike oil, which has several transportation options (Agerton and Up-

---

<sup>1</sup>IEA (2023a) estimates that oil and gas operations emitted 5.1 billion tons of CO<sub>2</sub>e in 2022, and IEA (2023b) estimates that flaring emitted around 0.5 billion tons of CO<sub>2</sub>e in the same year.

<sup>2</sup>The 20 and 100-year warming potential of methane are 81—83 and 27—30 times CO<sub>2</sub>. Source: EPA Website. “Understanding Global Warming Potentials.” Access June 2024.

<sup>3</sup>15063/1/21 REV 1 + REV 1 COR 1 + ADD 1.

<sup>4</sup>See 2 Colo. Code Regs. §404-1-903; N.M. Code R. §19.15.27 and §19.15.28; 89 FR 16820; and 89 FR 25378.

<sup>5</sup>Technically production data is available for natural gas at the well level and for oil at the lease level, which may contain multiple wells. For simplicity we use the term “wells” to refer to either natural gas wells or oil leases.

<sup>6</sup>In 2020, the Texas Permian Basin produced 3.4 mmbbl/d of oil (30% of the nation’s total) and 12.4

ton 2019; Covert and Kellogg 2017), gas transportation is limited to midstream pipelines. Further, when gas production approaches or exceeds the capacity of midstream infrastructure, constraints and congestion impede producers’ ability to send the gas to market. In this situation, they can flare gas to keep oil flowing. A recent survey found that almost half of industry executives said that low gas prices would not affect oil production decisions (Federal Reserve Bank of Dallas 2024, Special questions). Previous work has looked at flaring in the context of whether oil wells are connected to pipelines at all Lade and Rudik (2020) or from wells early in their production life. However, as shown in the lower pane of Figure 1, the majority of flaring in the Permian comes from wells already connected to pipelines, and the top pane of Figure 1 shows that a minority of that flaring comes from new wells (those with less than 12 months of production). Instead, responses to another survey of U.S. oil and gas executives point to midstream constraints as primary drivers of flaring (Federal Reserve Bank of Dallas 2019).<sup>7</sup> A similar pattern emerges globally: of flaring data provided by firms to the World Bank’s Zero Routine Flaring initiative, routine flaring only made up about one-third of total of reported flaring in 2022 (see Appendix Figure E.1). Because the estimated climate cost of flaring is approximately nine times the market value of the foregone gas in recent years, private markets undervalue midstream infrastructure to bring gas to market and flare more than is socially optimal.<sup>8</sup>

## 1.1 Empirical approach

Our analysis uses detailed data on pipelines, including unscheduled maintenance events; daily satellite readings of flaring and methane concentrations; and monthly production and flaring data for individual wells.<sup>9</sup> We examine the short-run impact of midstream congestion on flaring and methane emissions first at the aggregate level, and second at the well level.

Our main results leverage exogenous maintenance events on interstate transmission pipelines that temporarily reduced capacity. We estimate event studies capturing these effects. Then we examine the Henry Hub–Waha Hub price differential as a measure of congestion in transmission between the Permian and national demand. This price spread may be simultaneously

---

bcf/d of gas (11% of the nation’s total). However, Texas Permian oil was more valuable: producers reported nominal well-head oil revenues 5.5 times the gas revenues: \$127M/d versus \$23M/d. See Appendix Table E.1. National production data taken from EIA (US Field Production and Natural Gas Gross Withdrawals).

<sup>7</sup>Predominant factors cited in the survey include lack of transmission capacity, lack of processing capacity, gas processing fees exceeding the value of the gas, among others.

<sup>8</sup>In 2020 in the Texas Permian, firms reported flaring 0.26 bcf/d, valued at approximately \$0.50M/d at average wellhead prices. The social cost of flaring, though, was over eight times larger than the potentially foregone revenues at \$4.1M/d under a 95% flare efficiency. See Appendix Tables E.1 and E.3. Authors’ calculations.

<sup>9</sup>As we explain in Section 2.3, data in Texas is reported at the individual well-level for gas wells, but at the lease-level for oil-leases. We use the term “well” for generic discussion.

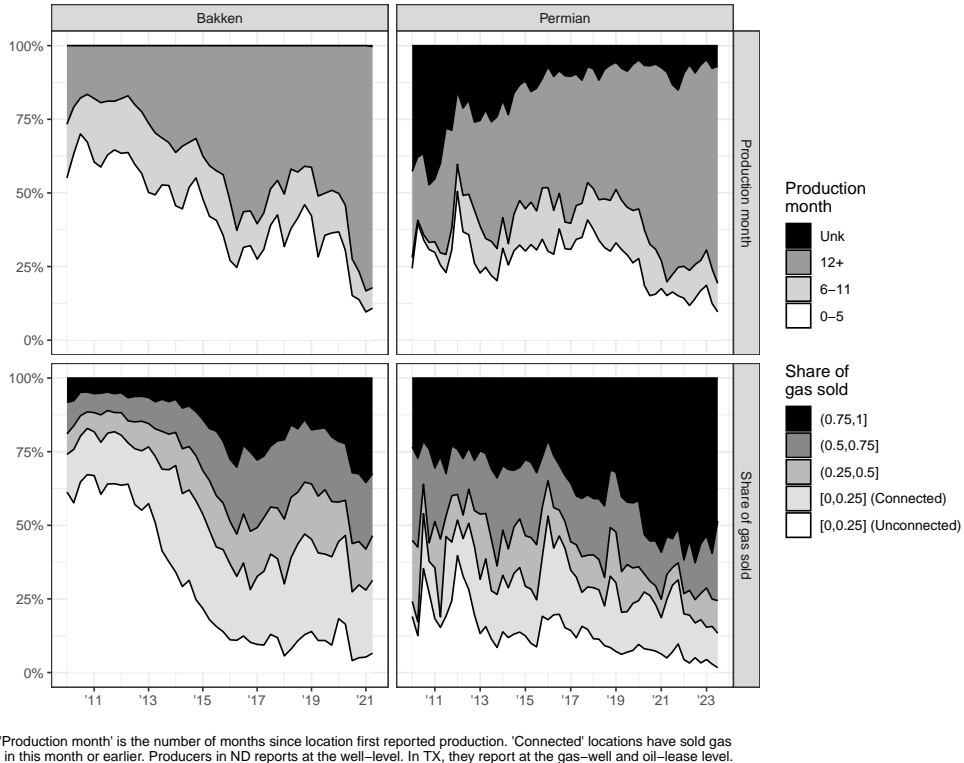


Figure 1: Attributed shares of flaring in the ND Bakken and TX Permian

determined with the amount of gas flared versus captured in the Permian. We therefore instrument using two sources of exogenous variation. First, we use our data on daily pipeline maintenance events to capture unexpected capacity shocks. Second, we construct a bespoke weather instrument that isolates inelastic demand shocks from the rest of the US that occur when storage inventories outside of Texas and New Mexico are unexpectedly low. These national demand shocks are met through increased utilization of gas transportation out of the Permian. This demand instrument could cause flaring because of pipeline congestion, or because of new well completions. We conduct several additional tests to rule out the second explanation. Using a variety of different spatial resolutions and an alternative event study framework, we find a consistent set of results. As transmission pipelines become congested, upstream flaring significantly increases, and both methane concentrations and methane emissions increase moderately.

We also examine how gas wells and oil wells respond to transmission constraints, comparing production, flaring, and sale prices following pipeline maintenance events. We find that gas wells and oil wells respond to capacity constraints in different ways. Gas wells mainly lower production, while oil wells maintain production and flare more. This aligns with the differing economics of gas versus oil wells. We also find evidence that vertically in-

tegrated wells are more responsive to maintenance events in terms of production and flaring, consistent with anecdotal evidence on the role of firm characteristics in flaring behavior.

## 1.2 Policy implications

Our estimates provide important insights for flaring and methane policy. First, our results suggest that focusing exclusively on routine flaring, as the new U.S. EPA (2024b) and the World Bank’s Zero Routine Flaring initiative do, although historically effective (Lade and Rudik 2020), will not mitigate future flaring as long as temporary flaring associated with congestion remains exempt. U.S. EPA (2024b) allows for up to 30 days of flaring “During temporary interruption in service from the gathering or pipeline system.” We estimate that congestion caused by transmission congestion caused 34 percent of flaring, but since our estimates may not incorporate congestion in gathering and processing, we view this as a lower bound. An upper bound on congestion-associated flaring is 90 percent, which is the share of flaring from connected Permian wells in the lower pane of Figure 1.

Second, we find that the climate costs of congestion-induced flaring and methane emissions are comparable in magnitude, yet newly proposed federal policy rules place much heavier emphasis on methane. For example, the new federal price on methane emissions from production (“Waste Emissions Charge”, or WEC) ignores the climate cost of CO<sub>2</sub> from flaring (U.S. EPA 2024c). Similarly, U.S. EPA (2024b) justifies flaring restrictions on the basis of methane emissions, not CO<sub>2</sub>. Our calculations in Appendix Table E.3 show, however, that revised estimates of the social cost of GHGs from U.S. EPA (2023) imply that the CO<sub>2</sub> component of flaring climate costs is now an order of magnitude larger than the methane climate costs at typical flare efficiencies used in EPA calculations (U.S. EPA 2024a).<sup>10</sup> The under-pricing of flaring relative to the efficient Pigouvian tax, combined with limitations on the monitoring and measurement of emissions (Agerton et al. 2023; Covert et al. 2024; Dunkle Werner and Qiu 2024) suggests complementary policies to reduce flaring could be warranted. Because midstream congestion causes joint production of flaring and methane emissions, policies to alleviate congestion may reduce both. Reductions can be achieved by increasing the quantity of midstream infrastructure, or decreasing the quantity of gas production. Our analysis does not show, however, whether flaring and methane emissions would be complements or substitutes in the absence of midstream congestion.

We show that when additional transmission capacity is made available for oil wells, there

---

<sup>10</sup>The 2020 SCC and SCM from IAWG (2021) report were \$51/ton and \$1500/ton under the then-baseline 3% discount rate (Tables A-1 and A-2). The 2020 SCC and SCM in the more recent U.S. EPA (2023) report are \$193/ton and \$1648/ton under the now-baseline 2% discount rate (Table A.5.1). Appendix Table E.3 applies these SCC and SCM estimates to calculate the climate costs of flaring. Prices are in 2020 dollars.

is a reduction in flaring but no corresponding increase in overall production in the short run. This contradicts the “fundamental law of road congestion” (Duranton and Turner 2011) which suggests that in equilibrium, new transportation capacity becomes congested. The contradiction indicates a need for future work examining the long-term impact of additional midstream infrastructure. Although our findings do not opine on the net climate benefits of long-run capacity expansions, our results have a potential policy implication regarding where to drill. For example, in regions with significant associated gas, policymakers might consider directing oil leases to be drilled in areas with more available midstream infrastructure or considering the timing of permitting alongside the availability of midstream infrastructure. This is particularly relevant for the U.S. Department of the Interior’s decision framework on where to conduct lease sales.

### 1.3 Related literature

Our paper contributes to several literatures related to infrastructure and the environment. First, our focus on the effects of midstream congestion is related to recent work on energy transportation infrastructure and environmental externalities from energy production. Similar to studies quantifying the importance of electricity transmission infrastructure for both the private and environmental values of renewable energy (Fell et al. 2021; LaRiviere and Lyu 2022), we find that the environmental value of natural gas depends on the infrastructure available to deliver it. In contrast to the electricity context with a single commodity (renewable energy), our setting is one of joint production as gas is often inelastically produced as a by-product of oil. Our findings demonstrate that gas can be an economic good or an environmental bad depending on midstream constraints.<sup>11</sup> One additional novelty is that previous literature has focused on methane leakage related to downstream infrastructure (Hausman and Muehlenbachs 2018) while we focus on upstream emissions caused by midstream congestion. A separate literature has also shown that energy transportation infrastructure (or its scarcity) can also lead to market power (Borenstein et al. 2000; Preonas 2019; Woerman 2019) and misallocation (Hausman 2024). This is certainly possible at a localized level in oil and gas (see discussion of the EXCO vs. Williams dispute in Agerton et al. (2023)).

Second, there is a large literature on the economic and environmental impacts of the growth in U.S. oil and gas production from shale, primarily focusing on impacts from upstream development. This literature is reviewed by Black et al. (2021). Our contribution is to causally identify how midstream congestion affects environmental externalities of upstream shale oil and gas development. Related to this, there is a growing literature on the

---

<sup>11</sup>This is somewhat distinct from studies quantifying the direct externalities from transporting energy commodities (Clay et al. 2017) or the impact of congestion on market efficiency (Oliver et al. 2014).

determinants and consequences of flaring (Agerton et al. 2023; Beatty 2022; Blundell and Kokoza 2022; Boslett et al. 2021; Fitzgerald and Stiglbauer 2015; Lade and Rudik 2020; Lau 2020; Thu 2023; Tran et al. 2024), although our focus on the midstream is unique. Our consideration of multiple pollutants is also consistent with recent discussions on accounting for co-pollutants in the economics literature (Stranlund and Son 2019; Zirogiannis et al. 2020).

Third, our paper contributes to the scientific literature on flaring and methane emissions. Scientific studies have suggested that a significant share of methane emissions may be associated with abnormal process conditions (Allen et al. 2015; Brantley et al. 2014; Mitchell et al. 2015; Zavala-Araiza et al. 2017, 2015) and unlit flares (EDF 2021; Plant et al. 2022), with previous correlational evidence linking midstream congestion (Lyon et al. 2021) to emissions. Our findings—that flaring and methane concentrations both rise when the midstream segment is congested—suggest that higher pressures and unexpected interruptions may be a root cause of abnormal process conditions that exacerbate emissions, and provide causal evidence to the previous correlational associations.

The rest of the paper is organized as follows. Section 2 describes our data sources. In Section 3, we present our analysis of how transmission pipeline congestion affects flaring and methane emissions at the basin level. Section 4 examines well-level responses to transmission constraints, comparing oil and gas wells. Finally, Section 5 discusses the implications of our findings and concludes.

Several online appendices provide additional details. Appendix A provides an overview of the industry for readers unfamiliar with it. Appendix B discusses a few details of our data construction, and Appendix C contains a theoretical model of pipeline capacity markets and constraints which motivates our empirical approach. Appendix D provides more detail and robustness checks for our IV, and additional results tables appear in Appendix E.

## 2 Data Sources

The focus of our study is the Permian Basin, which straddles Texas and New Mexico. Figure 2 shows an outline of the three main parts of the Permian: the gassier Delaware Basin is the western part, and the oilier Midland Basin is the eastern part. The two are split by the Central Basin Platform, which has somewhat less activity.<sup>12</sup> The map also shows the  $0.5^\circ \times 0.5^\circ$  degree cells we use later in our analysis. Our study combines five datasets on Permian pipelines, plants flaring, methane, and production from a mix of public and commercial sources. We note that our production data comes only from Texas.

---

<sup>12</sup>Outline provided by Enverus.

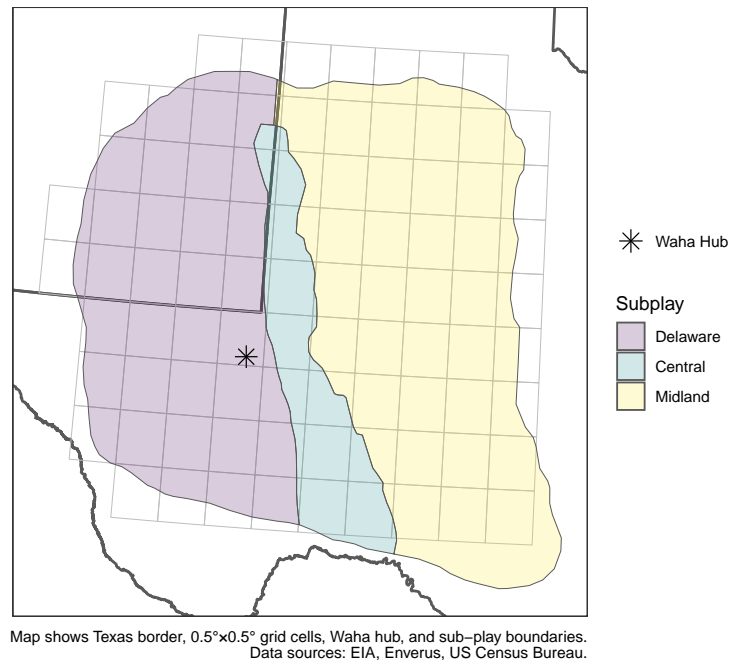


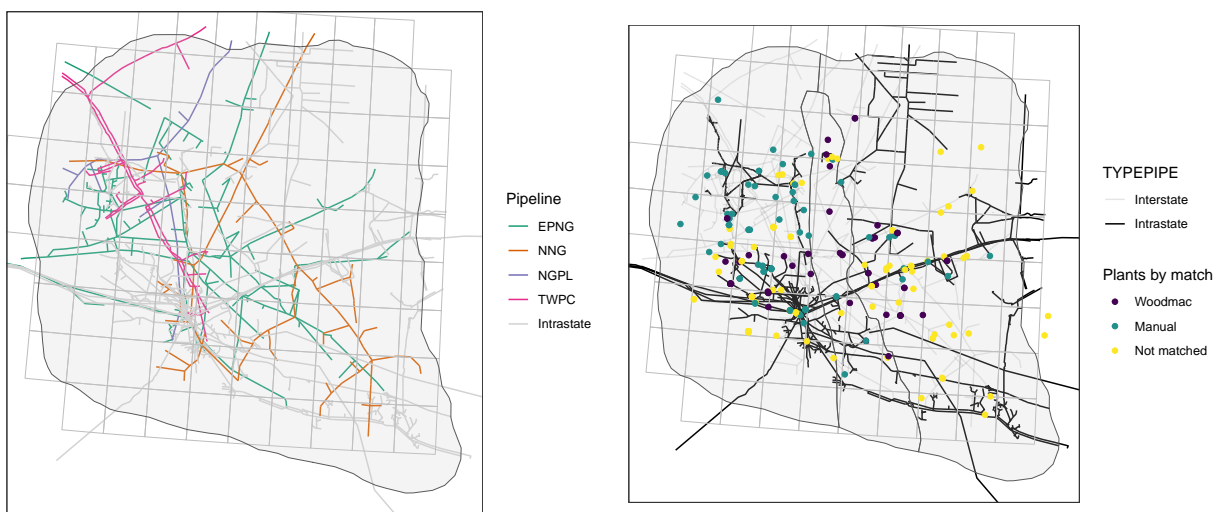
Figure 2: Map of Permian Basin

## 2.1 Interstate pipeline data

Our analysis focuses on interstate pipelines due to data availability. Interstate pipelines are regulated by the Federal Energy Regulatory Commission (FERC), which requires public disclosure of pricing and operational data. In contrast, intrastate pipelines in Texas are regulated by the Railroad Commission of Texas (RRC), which does not mandate such disclosures. We purchased historical data from Wood Mackenzie for the four interstate gas pipelines serving the Permian Basin: El Paso Natural Gas (EPNG), Natural Gas Pipeline Company of America, LLC (NGPL), Northern Natural Gas Pipeline (NNG), and Transwestern Pipeline Company (TWPC). The locations of these pipelines are illustrated in Figure 3a, along with intrastate pipelines that we do not have utilization data for.

Interstate transmission lines in the Permian form a network, and customers put in and take out natural gas at receipt and delivery nomination nodes. For each day, (9:00am to 8:59am the next day) shippers nominate volumes for receipt and delivery, and the pipeline schedules these (Mohlin 2021). Total nominations are made public and generally track actual receipts and deliveries. Operational capacity at nodes is also reported.

We follow Wood Mackenzie’s methodology to construct measures of utilization and total capacity for each pipeline by summing over subsets of nodes, and consulted with the com-



(a) Pipelines

(b) Plants

Figure 3: Permian infrastructure

pany about our data construction. We calculate net interstate natural gas receipts in the Permian each day by summing scheduled nominations over a list of nodes provided by Wood Mackenzie. We also calculate exports of natural gas from the Permian by summing over volumes through a few key operational chokepoints identified by Wood Mackenzie. These two quantities should be the same and, in general, track each other closely. In our analysis, we use exports since our receipts measure exceeds capacity for a short period on the Transwestern pipeline, but results are essentially unchanged if we use net receipts. We calculate the operational capacity of each interstate system to transport gas out of the Permian (“take-away” capacity) as the operational capacity at the export chokepoints. Time series of these three quantities—net receipts, exports, and operational capacity are depicted in Appendix Figure E.2.

Pipelines also post operational notices about when planned maintenance or unplanned outages impact operational capacity as well as *force majeure* events that allow the pipeline to interrupt services shippers have purchased. These events can be system-wide, or they can apply to particular segments and nomination points. We purchased a dataset of around 3,000 maintenance and unplanned outage events that Wood Mackenzie identified as important. Wood Mackenzie provides indicators of each event’s severity and whether it was planned or unplanned. One event states, for example:

*Northern will be conducting pipeline maintenance near the Spraberry, Texas, com-*

pressor station.... Northern will not sell any primary firm capacity from May 6 - 23, 2014 and the operational capacity of the point will be zero.

We keep only events that WoodMackenzie identifies as having “Significant,” “Major,” or “Severe” impact (versus “Little to no” or “Minor” impact) and events that impact East TX, West TX, or the Midcontinent. Appendix Figures E.4 and E.5 summarize the remaining 196 events and demonstrate that there is significant variation in these events both over time and across pipelines. A breakdown of the keyword frequency in these event descriptions shows that many events had to do with compressor station maintenance or malfunctions (Figure 4): Because pipeline investment is endogenously determined alongside firms’ drilling

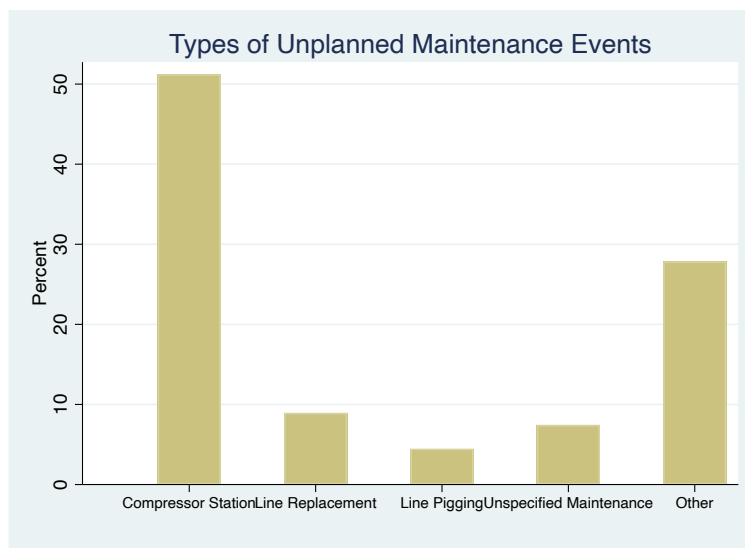
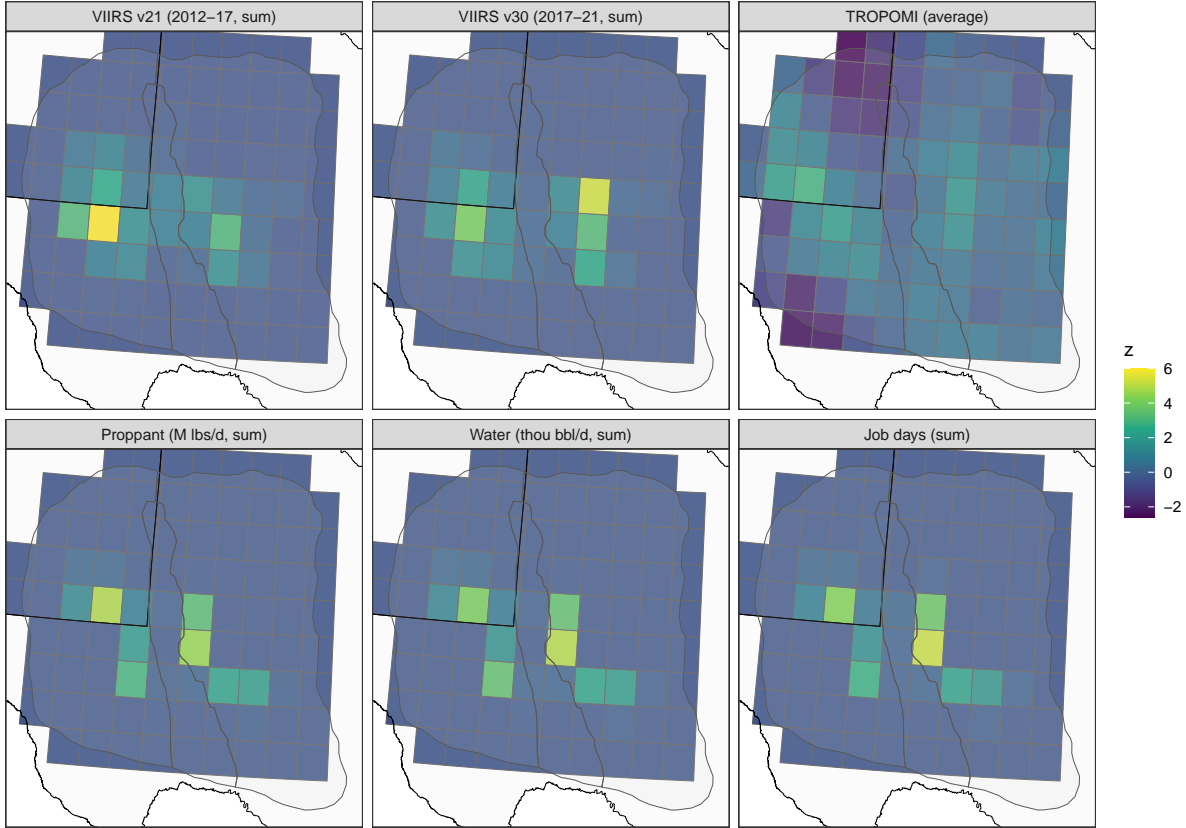


Figure 4: Keyword frequency in pipeline maintenance event descriptions

and production decisions (often years in advance), we use these operational events to identify unpredictable, short-run reductions in capacity on interstate pipelines. As we discuss later in Section 3, our identifying assumption is that specific interstate events are not correlated with either upstream firms’ production decisions or short-run capacity reductions on *intrastate* pipelines. While upstream producers and intrastate pipelines will generally expect some interstate maintenance and outage events to occur, we view the specific timing, location, and duration of events as randomly assigned.

## 2.2 Satellite data

We use two different satellite data products in our paper: one for flaring, and one for methane emissions. Both satellite products are generated at the daily level. For flaring, we use nightly flaring detections over the Permian Basin by the Visible Infrared Imaging Radiometer Suite



Summary of daily panel variables. State outlines and sub-play outlines are also visible. Variables are standardized by mean and std dev.

Figure 5: Aggregated daily satellite and fracking variables by grid-cell, standardized by mean and SD

(VIIRS) satellite instrument. VIIRS takes daily nighttime readings of radiant heat and light within the infrared band produced by natural gas flares. The VIIRS Night Fire (VNF) product we use provides measures of the temperature (K) and radiant heat (Watts). Gas flares are hotter than other heat sources like biomass fires, so we subset VIIRS data to detections with estimated temperatures greater than 1400K (Elvidge et al. 2016, 2013). We aggregate these individual flaring detections over the entire basin and over  $0.5^\circ \times 0.5^\circ$  grid cells. The top left and middle panel of Figure 5 show standardized sums of radiant heat for our VIIRS data over the periods 2012-17 and 2017-21.<sup>13</sup>

For methane emissions, we use daily readings from the satellite TROPospheric Monitoring Instrument (TROPOMI) aboard the European Union’s Sentinel 5-P satellite. TROPOMI measures methane concentration in columns of air globally. We use the concentrations provided in the Level 2 TROPOMI product (Hu et al. 2016, 2018). This TROPOMI product represents methane concentrations in units of column-average parts per billion, so values

<sup>13</sup>The VIIRS VNF products versions 2.1 and 3.0 cover different non-overlapping time periods, which we represent separately on this map. We sum the two products in our later analysis.

are not summable across space and time. Instead, we average them within  $0.5^\circ \times 0.5^\circ$  grid cells spanning the basin, or over the entire basin.<sup>14</sup> The top right panel of Figure 5 shows standardized average gridcell concentrations over our sample (May 2018–Sept 2021).

We would prefer to work with methane *emissions* (a flow) rather than *concentrations* (a stock) since this is the policy-relevant quantity. However, inverting concentration measurements into emissions is a challenging and computationally expensive task combining three-dimensional atmospheric chemistry and transport modeling that is beyond the scope of this paper. Instead, we construct an approximation to emissions based on the general structure of many of the popular inversion models in the scientific literature. This is described in Appendix B.2.

One advantage of using data from two different satellite instruments is that we can partially validate each data source with the other. TROPOMI and VIIRS take their readings from different satellites using different instrumentation (spectrometer for TROPOMI versus radiometer for VIIRS). Generally speaking, the same oil and gas production activities should lead to both flaring and methane emissions. We show in Appendix Table E.4 that we observe a strong relationship between detected flaring from VIIRS and detected methane concentrations from TROPOMI (and our emissions approximation). Although this relationship is not causal, i.e., we can’t say that flaring either avoids or causes higher methane emissions, it does provide evidence that these noisy satellite readings from separate instruments are capturing a signal from roughly the same ground-level phenomenon, rather than simply producing noise or spurious relationships.

## 2.3 Well data

Our last major source of data is monthly production data from Texas. One important feature of Texas reporting requirements is that gas wells report at the individual well level, while oil wells report as groups of wells at the “lease” level. For simplicity of exposition, we use the term “oil well” to refer to an oil lease. We merge both publicly available data from the Texas Railroad Commission (RRC) and commercial data-provider Enverus.<sup>15</sup> RRC data include oil and gas production data, as well as “disposition” data that include self-reported flaring. Enverus data include the same oil and gas production data (based on public RRC data) as well as information about the physical wells and their locations. Figure 6 shows the distribution of gas wells and oil leases across our study area. Producers in Texas report the

---

<sup>14</sup>We thank researchers Olga Khaliukova, Will Daniels, and Dorit Hammerling in the Applied Mathematics and Statistics Department at Colorado School of Mines for constructing this for us.

<sup>15</sup>Specifically, we use the Production Data Query (PDQ) Dump from the RRC and the “HPDI Raw Data Version 2: PDEN\_DESC.ALLOC\_PLUS” production data from Enverus.

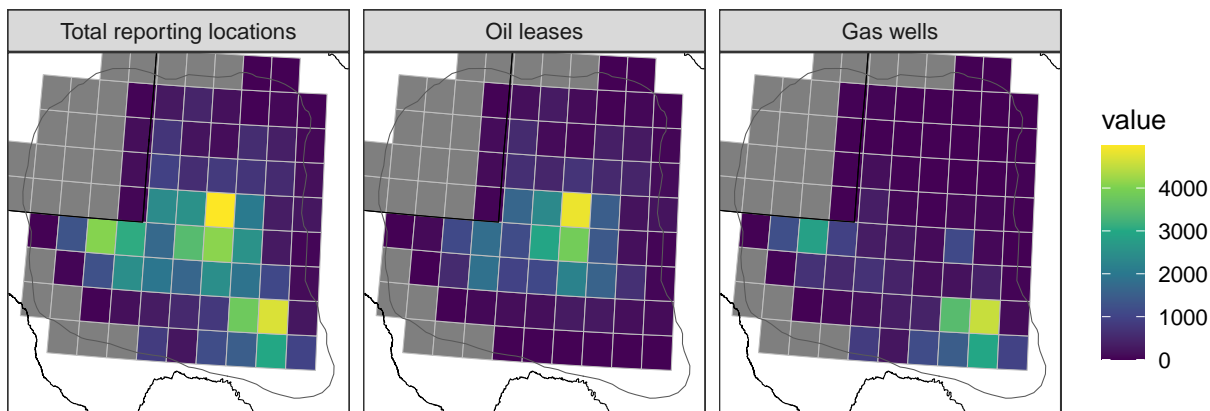


Figure 6: Counts of oil leases and gas wells in merged RRC/Enverus data by gridcell

volume and value of monthly sales to the Texas Comptroller. Enverus matches these sales data and includes them in our dataset. We use the ratio of value to volume to calculate an average wellhead price for each well-month. In some specifications of our daily panel analysis, we also include daily measures of ongoing hydraulic fracturing operations within each panel: the count of ongoing jobs and the sum of sand and water injected that day (bottom 3 plots in Figure 5). We downloaded these data from Enverus separately via the Enverus Developer API.

Our well-level analysis requires matching each gas well and oil lease to specific pipelines. We accomplish this by first matching each to its closest processing plant using the shortest distance along the gathering pipeline network. We purchased data on gathering pipelines in Texas from commercial provider MapSearch for the year 2019,<sup>16</sup> and we purchased processing plant data from Wood Mackenzie. Details of our matching methodology can be found in Appendix B.1.

## 2.4 Other data

For our analysis in Section 3, we use the natural gas spot price at the Waha trading hub located in the Delaware Basin within the Permian (marked in Figure 2), and Henry Hub in Louisiana, which is a nationally representative North American benchmark natural gas price. The difference in the Henry Hub and Waha prices represents the shadow value of transmission

<sup>16</sup>We contacted several commercial data providers as well as the RRC. With the exception of MapSearch, none maintained historical versions of the data. When we purchased the data, the 2019 year was the most recent version available. We also purchased a 2008 version of the pipeline data, though we do not use it in this analysis.

capacity between the two hubs and serves as a measure of constraints to moving gas out of the Permian.

For our analysis in Section 3 we use state-level heating and cooling degree-days from NOAA and 2010 state-level population data from the Census Bureau. We use this weather information to construct a population-weighted measure of unexpected previous gas demand associated with weather shocks.

### 3 Transmission Pipelines

We study how congestion on transmission pipelines impacts flaring and methane emissions. We use two primary measures of congestion, and we perform analyses on both aggregate, basin-level time series as well as a panel of grid cells spanning the Permian basin. We first estimate a series of event studies examining how discrete, unplanned maintenance events reduce total pipeline operational capacity and thereby impact flaring and methane. These event studies, however, do not allow us to estimate how pipeline congestion (as measured on a continuous scale) impacts flaring and methane. This limits our ability to perform counterfactuals, so we next causally estimate how flaring and methane concentrations respond to a continuous measure of congestion.

#### 3.1 Event studies

**Pipelines capacity and throughput** For the event studies, we let time be indexed by  $t$  and generate a set of dummy variables  $\mathbb{1}_{jt}$  that take a value of one if there is at least one event that begins at time  $t$  on interstate pipeline  $j$ . For this analysis, we consider the four primary interstate pipelines of the Permian where data is available during our sample time period, El Paso Natural Gas, Northern Natural Gas, Natural Gas Pipeline Company of America, and Transwestern Pipeline Company. Our event study model is:

$$Y_{jt} = \sum_{\tau=-3}^3 (\beta_{\tau} \cdot \mathbb{1}_{j,t+\tau}) + X'_{jt}\alpha + \eta_j + \delta_{month(t)} + \varepsilon_{jt}, \quad (1)$$

where  $Y_{jt}$  is the log of either operational capacity or scheduled exports (throughput) on day  $t$  on pipeline  $j$ . We normalize with respect to the day prior by setting  $\beta_{-1} = 0$ , so that each coefficient  $\beta_{\tau}$  represents the difference in the outcome between day  $t + \tau$  and the day prior to the event ( $t - 1$ ). The row vector  $X'_{jt}$  contains a constant and pipeline time trend. We include pipeline-specific dummies  $\eta_j$  to control for average pipeline capacities and throughput, as well as month-of-sample fixed effects  $\delta_{month(t)}$ . Standard errors for this

pipeline analysis are clustered at the pipeline-month level. While firms probably expect disruptions in transmission to occur, we assume that they are unable to predict the specific timing, location, and duration of specific events. Under this assumption, maintenance events are exogenous to firms’ production decisions, and our estimates have a causal interpretation.

Our initial step is to show that maintenance events affect pipeline capacity and throughput. We focus on 173 of our 196 unplanned events since the event windows are “clean,” so that no other event is ongoing within a three day window before and exclude any post event days where a new event begins. This leaves us 1,114 pipeline-day observations. Figure 7 plots estimated coefficients  $\hat{\beta}_\tau$  for these event studies of log throughput and log capacity (1), along with their 90% confidence intervals. Figure 7b shows a 14.6% drop in operational capacity on the day the event begins ( $\tau = 0$ ), with an estimated impact of 4.3% on the day following ( $\tau = 1$ ) that is statistically significant at the 10% level. Figure 7a shows similar throughput declines of 14.7% and 4.7% for the first two days of the events, with these estimates statistically significant at the 10% and 5% level.<sup>17</sup> Because average operational capacity is larger than average throughput (0.46 bcf/d versus 0.35 bcf/d), the impact on total operational capacity is larger than the estimated effect on total throughput. The noisier estimate for a drop in capacity is not entirely surprising due to the construction of our data. Our operational capacity is measured at a few, discrete network nodes that serve as “chokepoints.” The capacities at these chokepoints, however, may not always reflect constraints at upstream receipt points that limit throughput and are the relevant binding constraints.

**Flaring and methane** We now turn to estimating how maintenance events impact satellite measures of flaring, methane concentrations, and methane emissions. We report analysis at the daily level, although results are robust to aggregating to the weekly level. The model we estimate is similar to (1), with the difference that we use a single time series (and therefore drop pipeline fixed effects):

$$Y_t = \sum_{\tau=-3}^3 (\beta_\tau \cdot \mathbb{1}_{t+\tau}) + X_t' \alpha + \varepsilon_t. \quad (2)$$

Here,  $Y_t$  is either log flaring, log methane concentrations, the level of methane emissions, or the log of emissions. We measure flaring as the log of the sum of the radiant heat from VIIRS flare detections over the entire Permian Basin, and we measure log methane concentrations and log emissions as described in Section 2.2 and Appendix B.2. We estimate equation 2 by

---

<sup>17</sup>Appendix Table E.9 displays these results as well as a robustness check in which we estimate the model separately for NGPL—which has about half of the “clean” events—and the other three pipelines. This check suggests that our results are not driven by one particular pipeline.

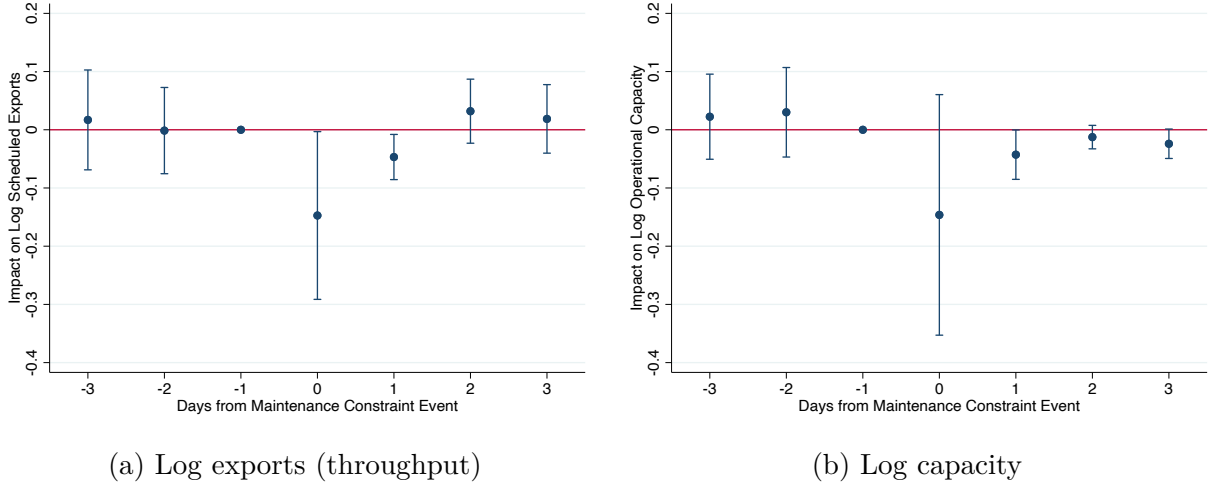


Figure 7: Event study results for the effect of pipeline maintenance events on interstate pipeline’s operational capacity and throughput (exports) at the daily frequency. The regressions control for pipeline fixed effects, month fixed effects, and linear pipeline time trends. Plots show estimated  $\hat{\beta}_\tau$  from (1) along with 90% confidence interval error bars.

OLS for log methane concentrations and methane emissions levels, and by Poisson regression for log flaring and log methane emissions in order to handle days with zeros in our satellite flaring data or our methane emissions calculations. The indicator variable  $\mathbb{1}_t$  takes a value of one if there is an event on day  $t$  on any of the four interstate pipelines. The vector  $X_t$  includes a constant and a trend in the flaring regressions, with monthly seasonal dummies included in the methane regressions to control for seasonality in atmospheric methane from natural sources. Results are robust to dropping the trend, to controlling for daily fracking activity using the number of fracking jobs and the daily quantity of fracking water and proppant used, and to using OLS with levels or logs for all outcome variables (with dropped observations for zeros in the logged outcomes). Coefficients from the main event study specifications are reported in Appendix Table E.5, with robustness checks reported in Appendix Tables E.6 and E.7.

Figure 8 shows the results from these four event studies from equation (2). Each panel contains no evidence of statistically significant pre-event trends. They indicate that maintenance events lead to statistically and economically significantly higher flaring, methane concentrations, and methane emissions. Flaring increases by about 65% on the day of an unplanned maintenance event, relative to the previous day (Figure 8a). Although this may seem large, the mean and standard deviation of flaring levels are fairly close, so that a 65% increase relative to the mean is approximately 0.61 standard deviations. (Summary statistics are in subcaptions of Figure 8). Methane concentrations, by contrast, increase by about 0.53% (Figure 8b). With a mean of 1864 and standard deviation of 18.2 parts per billion,

this amounts to an effect of about 0.5 standard deviations. The relative size of the methane emissions impact is fairly similar whether measured in levels (Figure 8c) or logs (Figure 8d): with an increase of approximately 60 tons of methane emissions per day, this is a little more than 0.5 standard deviations. At EPA’s 2020 SCM of \$1,648/t, 60 tons amounts to almost \$100,000 in methane-related climate costs per day of unplanned maintenance event.

## 3.2 Continuous congestion measure

Our initial event studies are helpful in demonstrating that unexpected reductions in pipeline capacity cause increases in flaring and methane. However, they do not identify the elasticity of flaring and methane emissions with respect to congestion on interstate transmission, which we need in order to understand how flaring and methane emissions would have evolved absent congestion.

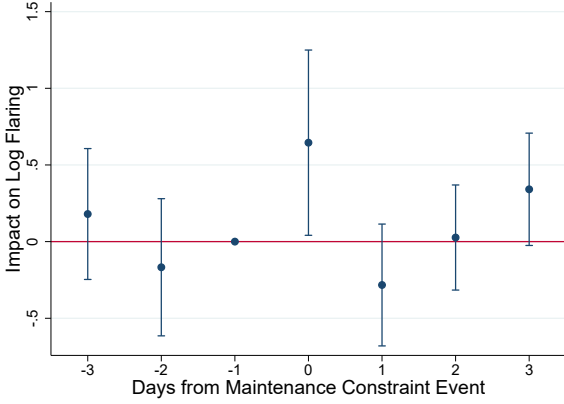
Since we lack visibility into intrastate pipeline capacity and utilization—which make up a large share of transportation out of the Permian—we cannot construct a physical measure of total pipeline utilization or congestion. Instead, we use the the difference between natural gas prices at Henry Hub in Louisiana and the Waha hub (marked in Figure 2) in the Permian Basin. This price differential is a measure of system-wide transportation congestion on gas transmission that moves gas both within the Permian and away from it. The differential rises with congestion and scarcity of pipeline capacity (Agerton and Upton 2019; Cremer and Laffont 2002; Oliver et al. 2014). At times when there are no transportation constraints, the price of natural gas in the two locations move in tandem. But when prices in Waha fall significantly relative to Henry Hub, this represents a transportation bottleneck between the two hubs. Figure 9 plots the Henry–Waha price differential and interstate pipeline utilization from 2016 to 2021.<sup>18</sup> The correlation between the two (0.62) is clear visually.

A simple linear regression of flaring or methane on the Henry–Waha price differential may not have a causal interpretation for the standard reasons that a regression of quantities on prices may not. First, there is potential for simultaneity bias as the price differential is simultaneously determined with production and emissions. Second, we cannot rule out the possibility of bias from the presence of an omitted variable that influences both a producer’s decision to flare and the willingness to pay for gas.

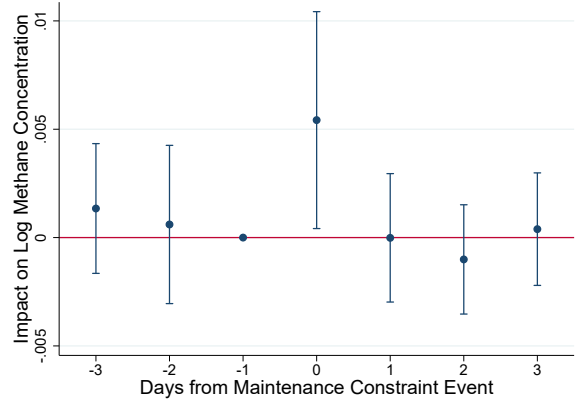
In order to address these concerns, we instrument for the price differential using (a) our maintenance events that reduce interstate pipeline capacity, and (b) unexpected shocks to

---

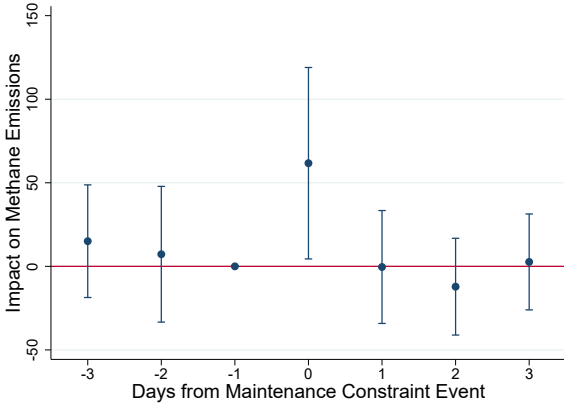
<sup>18</sup>We calculate interstate pipeline utilization using Wood Mackenzie’s methodology. We define utilization as the sum of scheduled exports divided by the sum of operational capacity at designated chokepoints.



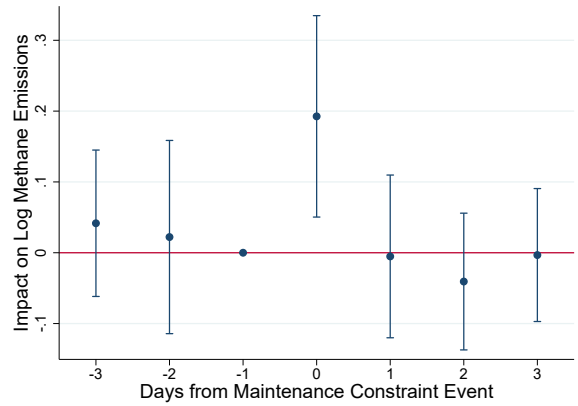
(a) Log flaring  
 $\mu=169.8, \sigma=181.5$



(b) Log CH<sub>4</sub> concentration  
 $\mu=1864, \sigma=18.7$



(c) CH<sub>4</sub> emissions  
 $\mu=277.7, \sigma=112.9$



(d) Log CH<sub>4</sub> emissions  
 $\mu=277.7, \sigma=112.9$

Figure 8: Event study results for the effect of pipeline maintenance events on flaring, methane concentrations, and methane emissions at the daily frequency. The flaring regression in Panel (a) controls for a linear trend, while the methane regressions in Panels (b) to (d) control for a linear trend and monthly dummies. Panels (b) and (c) are estimated by OLS, and Panels (a) and (d) are estimated by Poisson regression. Error bars are 90% confidence intervals.  $\mu$  and  $\sigma$  represent the mean and standard deviation of the levels of each variable in the estimation sample. The units for the levels of flaring radiant heat are in watts; the levels of methane concentration are in parts-per-billion; and the units of methane emissions are in tons.

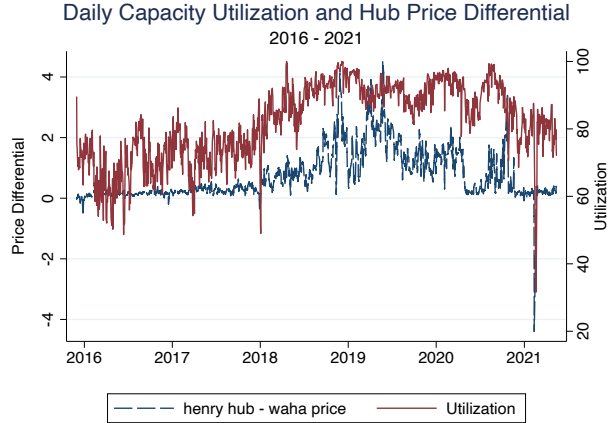


Figure 9: Henry–Waha price differential and interstate pipeline capacity utilization (scheduled exports divided by chokepoint operational capacity)

out-of-state demand that occur when out-of-state storage inventories are unexpectedly low. These gas demand shocks in the rest of the US increase demand for transportation out of the Permian basin because they cannot be satisfied by storage withdrawals in their local market. Having this separate instrument helps confirm that congestion-induced emissions do not simply result from the maintenance events themselves (for example, blowdowns at compressor stations), but induces emissions across the broader natural gas system. The identifying exclusion restriction for both instruments is that our instruments only affect flaring and methane emissions via their effects on the price differential, which represents an implicit price of transmission capacity. We construct our maintenance event instrument  $Z_{1t}$  as the existence of an active maintenance event on a given day— $\mathbb{1}_t$  in (2). Our event study supports the exclusion restriction for  $Z_{1t}$  as an instrument. Figure 8 contains no evidence for a statistically significant difference in pre-event trends for flaring or methane. If there were a set of unobserved variables that correspond with both emissions and the occurrence of these events, then one would expect to observe differential emissions prior to the event.

Our demand shock instrument  $Z_{2t}$  isolates variation in weather that creates unexpected demand for gas transportation from the Permian during conditions of depleted storage in the rest of the country. We construct this IV using cumulative unexpected weather shocks over the preceding year in all lower 48 US states that do not border Texas or New Mexico. We residualize heating and cooling degree days in the rest of the US with a regression on monthly dummies, time trends, and a time lag. The residuals are daily unexpected out-of-state demand shocks. We take the cumulative sum of these residuals over the preceding 365 days and build a single variable  $Z_{2t}$  (see details in Appendix D.1). These cumulative unforecasted weather shocks capture the unexpected portion of gas storage inventory depletion.

The mechanism behind this IV is that rights to pipeline capacity are either firm or interruptible. In response to national gas demand shocks, Permian operators that hold gas inventories may reroute them to the interstate pipeline system in order to satisfy national demand. Those with interruptible rights would then lose pipeline space and may be induced to flare and/or emit methane. Appendix Section C develops a model that describes the interruptible capacity market under congested conditions as a lottery. In response to national demand shocks, the value of the interruptible capacity lottery increases. More local firms try to sell to the national market, but a smaller share of them are able access the pipeline. Local prices may increase as more firms try to access the national market. However, because of congestion, local prices increase by less than the national price shock, and the differential widens. The model predicts that during a constrained time, both national demand shocks and decreases in pipeline capacity can widen basis differentials and can increase flaring.

The exclusion restriction for this IV is that the previous year’s worth of unforecasted weather-driven storage depletion in Utah or Tennessee, for example, should not affect flaring or methane emissions in the Permian basin on a given day except through its effect on congestion. One concern with this assumption might be that Permian producers respond to these demand shocks by initiating new production, which can cause upstream flaring and methane emissions irrespective of midstream congestion. This is unlikely to be driving our results for several reasons.

First, initiating new production takes time and is done based on expectations about future demand. We isolate shocks that were unexpected as the residuals of a weather forecasting regression, and we use daily variation over which time it is unlikely that new wells can be brought online in response to unexpected demand shocks on the same day. Second, we show in Appendix D.2 that, although  $Z_{2t}$  is positively correlated with our fracking activity variables (daily number of active fracking jobs, daily quantities of fracking water and proppant) over low levels of  $Z_{2t}$  when the pipeline system is less congested, they are uncorrelated or negatively correlated over moderate to high levels of  $Z_{2t}$  when the pipeline system is more congested.<sup>19</sup> Similarly, we show that at low levels of congestion,  $Z_{2t}$  drives the local Waha price down but has a small positive effect on the Henry Hub price. In contrast, at moderate-to-high levels of congestion, it has a null or positive effect on Waha and a larger positive effect on the Henry Hub price. These stylized facts suggests that there may be some limited supply increase when pipelines are not congested, but that over the variation we are interested in—congested conditions— $Z_{2t}$  is predicting increases in congestion but not increases in supply. In a constrained environment, these positive effects on individual prices

---

<sup>19</sup>This is also consistent with our findings at the well-level analysis in Section 4 that gas wells reduce output in response to congestion but oil leases do not.

with a widening differential are also consistent with our model’s predictions in Appendix C. Third, in order to validate the previous point, we report results in Appendix D.2 that control for the daily fracking activity controls in the second stage of our IV regressions so that production responses are not in the residual, and we estimate heterogeneous responses under congested and uncongested conditions. The results of these robustness checks are consistent with our main results, and a more thorough evaluation of the relevance and validity of this IV is presented in Appendix D.2.

We estimate the impact of congestion (price differential) on flaring and methane using

$$Y_t = \beta_0 + \beta_1 \Delta p_t + X_t' \alpha + \varepsilon_t \quad (3)$$

where  $\Delta p_t$  is the price differential, which we instrument using  $Z_{1t}$  and  $Z_{2t}$ . Table 1 presents the estimates of  $\beta_1$  with the regional price differential as our measure of congestion using OLS as well as IV with different combinations of instruments. In Panels A–D, the dependent variables are log flaring, log methane concentrations, methane emissions, and log methane emissions. Column (1) shows the OLS results for reference. Column (2) uses only the maintenance event IV  $Z_{1t}$ , and Column (3) uses only the cumulative weather-driven storage depletion IV  $Z_{2t}$ . Column (4) uses both IVs.

For all outcome variables, the OLS estimates in Column (1) are smaller than any of the IV estimates. This is consistent with flaring and methane emissions being a form of free disposal of excess natural gas: when the transportation system is constrained, a unit of methane that is not flared or emitted is sold into the Waha hub, driving down the local price and driving up the price differential. This reverse causality works in the opposite direction of the congestion effect we are attempting to estimate, biasing our coefficients downward. The maintenance event IV  $Z_{1t}$  in Column (2) produces the largest coefficients in each panel, but also the largest standard errors and the smallest Kleibergen-Paap first-stage F-statistics (KP-F). The KP-F statistic for this IV is only above the “rule of thumb” cutoff of 10 in the flaring regression, suggesting that this is not a strong instrument. The cumulative weather IV  $Z_{2t}$  in Column (3) is the strongest IV, by contrast, with much larger KP-F statistics. The models in column (4) are overidentified, permitting a Hansen’s J-test of instrument exogeneity, which all four models pass. Our results are robust to including daily activity controls for the number of active fracking jobs and the amount of water and proppant used in fracking. Overall, the pattern and the magnitudes are consistent with our event study estimates.

Our methane impacts (Panels B–D) are less precisely estimated than our flaring impacts. There are two explanations for this. First, our satellite methane data begins later than

Table 1: Impact of Henry Hub-Waha Price Differential on Flaring and Methane: Time Series

	OLS	$Z_{1t}$	$Z_{2t}$	$Z_{1t}, Z_{2t}$
<b>Panel A: Log Flaring</b>				
$\Delta p_t$	0.63*** (0.059)	0.98*** (0.23)	0.77*** (0.093)	0.78*** (0.093)
$R^2$	0.25	0.22	0.24	0.24
KP - F Stat		12.7	58.6	50.5
Hansen's J p-value				0.31
N = 1278				
<b>Panel B: Log Methane Concentrations</b>				
$\Delta p_t$	0.00034 (0.00038)	0.0076 (0.0083)	0.0017 (0.0011)	0.0018* (0.0011)
$R^2$	0.48	0.28	0.47	0.47
KP - F Stat		1.62	26.7	15.0
Hansen's J p-value				0.33
N = 715				
<b>Panel C: Methane Emissions</b>				
$\Delta p_t$	2.77 (3.96)	87.2 (94.9)	15.4 (11.5)	17.5 (11.4)
$R^2$	0.51	0.28	0.50	0.50
KP - F Stat		1.62	31.5	16.6
Hansen's J p-value				0.30
N = 715				
<b>Panel D: Log Methane Emissions</b>				
$\Delta p_t$	0.074*** (0.025)	0.43 (0.51)	0.23*** (0.084)	0.24*** (0.082)
$R^2$	0.42	0.28	0.39	0.39
KP - F Stat		1.83	24.9	14.7
Hansen's J p-value				0.65
N = 699				

**Notes:**  $\Delta p_t$  is the Henry Hub - Waha price differential. All regressions include a linear trend and monthly dummies. Panel A reports results for the log of flaring, Panel B for the log of methane concentrations, Panel C for methane emissions, and Panel D for the log of methane emissions. Column 1 reports OLS estimates. Column 2 uses  $Z_{1t}$ , the presence of a pipeline maintenance event, as an IV for  $\Delta p_t$ . Column 3 uses  $Z_{2t}$ , the cumulative unexpected weather shocks proxying storage depletion, as an IV. Column 4 uses both IVs. HAC standard errors in parentheses. \*\*\* indicates significance at the 1% level, \*\* at the 5% level, \* at the 10% level.

our flaring time series, so there are fewer observations in the methane regressions. This may reduce the precision of the methane estimates and statistical significance. Second, there may be measurement error associated with the TROPOMI instrument, the processing algorithms, and our inversion, which could all cause lower precision.<sup>20</sup>

Overall, our time series estimates in Table 1 show that long-range transmission pipeline congestion leads to statistically significant increases in upstream flaring, and noisy but economically important increases in upstream methane emissions in the Permian. Our preferred estimates in column (4) indicate that a \$1 increase in the price differential raises flaring by 78 percent, methane concentrations by 0.18 percent, and methane emissions by 17.5 tons or 24 percent.<sup>21</sup> The average price differential during our sample period (2015–2021) was \$0.433/mcf. Average flaring levels were 97.1 bcf/yr according to our calculations from RRC data, and methane emissions were 3.94 million tons/yr according to Varon et al. (2023). Given our coefficient estimates of 0.78 and 0.24 in Panels (A) and (D), this implies that congestion accounted for 34% of flaring and 10% of methane emissions. Under the 2020 SCC and SCM, congestion-induced flaring imposed around \$524 M/yr in global climate costs, and congestion-induced methane, around \$674M/yr.<sup>22</sup>

### 3.3 Grid cell panel estimates

The Permian Basin is not a homogeneous producing region, and there may be highly localized changes in production activity and land use that affect methane concentrations differently over space and time. Wetland off-gassing and agricultural activity are important sources of methane emissions which may have different seasonal behavior or long-run trends in different

---

<sup>20</sup>We also note that there are also fewer observations in Panel D than in Panels B or C because there are days with zero methane emissions calculated in our conversion method from concentration to emissions. There are also a few days with zero flaring detections by the VIIRS instrument. When we include these zero observations and estimate a Poisson IV regression using the control function approach of Lin and Wooldridge (2019), we find similar statistically significant impacts on flaring of 70 percent rather than 78 percent, and on methane emissions of about 18 percent rather than 24 percent.

<sup>21</sup>The average price differential over the period for which we have methane data is \$1.05 whereas the standard deviation is \$0.83, so these interpretations reflect typical variation during the study period.

<sup>22</sup>In order to arrive at these social cost figures, we multiply the average price differential (\$0.433) by the estimated increase in flaring ( $0.78 \times 97.1 = 75.8$  bcf/yr) or methane emissions ( $0.24 \times 3.94 = 945,000$  metric tons/yr), and further multiply these by the 2020 social cost of flaring (\$15.96/mcf) or methane (\$1648/ton) expressed in 2020 dollars. Our climate cost of flaring assumes 95% combustion efficiency using an associated gas mix from Howard et al. (2015) (see Appendix Table E.3). We use the 2020 social costs in order to represent social costs incurred during our sample. Applying updated 2024 social cost figures measured in 2020 dollars (\$208/t<sub>CO<sub>2</sub></sub> and \$1950/t<sub>CH<sub>4</sub></sub>, which together raise our social cost of flaring to \$17.32/mcf) would bring these estimates to \$568M/yr in global climate costs from congestion-induced flaring, and \$798M/yr from congestion-induced methane. It is also worth noting that these methane social cost estimates rely on the full, state-of-the-art atmospheric inversion model in Varon et al. (2023), so that errors in our approximate conversion from methane concentration to emissions should not alter the scale of our estimated social costs.

parts of the basin. By using aggregate daily averages of basin-wide methane concentrations in the time series analysis, we are including much of this unwanted variation without controlling for it. In order to flexibly control for these localized unobserved changes across seasons and across years, we divide the Permian Basin into the  $0.5^\circ \times 0.5^\circ$  grid cells shown in Figures 2 and 5.<sup>23</sup> We index cells by  $c$  and use daily average methane concentrations within each cell (along with derived daily total methane emissions, and daily total flaring within each cell) in order to estimate a series of models akin to (3) with cell-by-month fixed effects to control for local cell-level seasonality associated with different non-oil-and-gas land uses, and cell-by-year fixed effects to control for local cell-level trends in oil and gas or other land uses. Our estimating equation is

$$Y_{ct} = \beta D_{ct} + \alpha_{c,year(t)} + \gamma_{c,month(t)} + \epsilon_{ct} \quad (4)$$

where  $\alpha_{c,year(t)}$  are cell-by-year fixed effects,  $\gamma_{c,month(t)}$  are cell-by-month fixed effects, and  $D_{ct}$  is our measure of congestion (the price differential or maintenance event indicators).

First, we reexamine the impact of the price differentials setting  $D_{ct} = \Delta p_t$  and instrumenting using  $Z_{1t}$  and  $Z_{2t}$  as we did for (3). Second, to more clearly identify the transportation constraint channel, we use information on which of the four interstate pipelines had an unplanned maintenance event on a given day, and how much of each grid cell’s natural gas processing capacity feeds each pipeline. As Figure 3b shows, some cells have multiple processing plants clustered together, whereas other areas have few or none. We have also matched plants to pipelines. If the majority of a grid cell’s processing capacity is associated with one pipeline, then unplanned maintenance events on that pipeline may have a larger effect on flaring and methane emissions in that cell than on another cell in which no processors are supplying the affected pipeline. Therefore we also estimate models in which  $D_{ct}$  is the weighted average of dummies for unplanned maintenance events on individual pipelines, where weights are the share of cell  $c$ ’s processing capacity that typically supplies gas to each pipeline.<sup>24</sup> Define an event impacting cell  $c$  at time  $t$  as

$$D_{ct} \equiv \sum_{j \in \text{pipelines}} w_{cj} \times \mathbb{1}_{jt}$$

where  $w_{cj}$  is the share of gas processing capacity in cell  $c$  served by interstate pipeline  $j$ .<sup>25</sup>

---

<sup>23</sup>The top right panel of Figure 5 shows standardized average gricell concentrations over our sample (May 2018–Sept 2021).

<sup>24</sup>If a processing plant cannot be linked to a specific pipeline, we allocate its share of the cell’s capacity to a dummy representing the existence of an event on any pipeline. Results are robust to calculating share weights using only plants linked to a specific pipeline.

<sup>25</sup>The results are robust to alternative weighting schemes, such as using each pipeline’s share of total

Table 2 shows results from these panel regressions using  $\Delta p_t$  instrumented with  $Z_{1t}$  and  $Z_{2t}$ . Results are generally consistent with the time series results in the previous subsection, with much higher first-stage KP-F statistics in each regression. Estimated impacts on flaring are somewhat lower but still of the same order of magnitude and still highly statistically significant. The estimate may be smaller because we are now estimating the average impact across both low- and high-flaring cells rather than the total basin-wide impact. By contrast, the methane estimates are much more clearly statistically significant now that we are more flexibly controlling for cell-level trends in average concentrations. However, the magnitude of the effect on methane emissions—18 percent—is fairly similar to the time series estimate of 24 percent in the log regression, and the impact in the levels regression of about 15 tons per dollar of price differential is very close to our time series estimate, but now highly statistically significant.

Table 2: Impact of Henry Hub-Waha Price Differential on Flaring and Methane: Grid Cell Panel

	Flaring (Poisson)	Log Methane Concentration	Methane Emissions	Log Methane Emissions
$\Delta p_t$	0.19*** (0.067)	0.0088*** (0.0012)	15.4*** (1.70)	0.18*** (0.013)
N	37204	39082	39099	36896
N cells	88	88	88	88
KP-F	83829	334.9	20979	17505

**Notes:**  $\Delta p_t$  is the Henry Hub - Waha price differential. All regressions include cell-by-month and cell-by-year fixed effects. Column (1) is a panel Poisson IV regression using the control function approach of Lin and Wooldridge (2019) to account for many cells with zero flaring, whereas Columns (2) to (4) are panel IV regressions. All three columns use  $Z_{1t}$ , the presence of a pipeline maintenance event, and  $Z_{2t}$ , the cumulative unexpected weather shocks proxying storage depletion, as IVs. Standard errors are clustered at the cell level. \*\*\* indicates significance at the 1% level, \*\* at the 5% level, \* at the 10% level.

Table 3 shows results from these panel regressions using processing capacity-weighted pipeline maintenance events. For comparison, Panel A shows results using a dummy variable transportation capacity or each cell’s share of total Permian processing capacity. While we also find similar results when weighting  $\Delta p_t$  by local processing capacity shares, we present the simpler unweighted version for clearer interpretation.

for any event whereas Panel B shows the results of weighted events. For each outcome, the treatment effects roughly double or triple when we weight by grid-cell processing capacity serving the impacted pipeline. Interestingly, comparing grid cell IV results in Table 2 to grid cell event results in Panel B of Table 3 shows that the flaring impacts from a processing-weighted pipeline event are similar in magnitude to a \$1 increase in the price differential (25 percent vs. 19 percent), but the upstream methane impacts from pipeline events are as much as an order of magnitude smaller than from a \$1 price differential change. This could be because discrete adverse events like unplanned pipeline maintenance are announced and trigger operators to take actions like lighting flares to mitigate the event whereas weather-driven variations in price differentials do not have direct operational impacts. Operators may respond to discrete events by purposefully flaring and thereby reducing accidental methane emissions whereas the impact of system-wide congestion may occur through multiple channels including flaring and venting but also leaking that operators are not aware of.

Table 3: Impact of Cell Processing-weighted Pipeline Events on Flaring and Methane: Grid Cell Panel

	Flaring (Poisson)	Log Methane Concentration	Methane Emissions	Log Methane Emissions
Panel A: Any Event ( $w_{ip} = 1$ )				
$\beta$	0.075*** (0.022)	0.00029*** (0.000094)	1.18 (0.95)	0.0072 (0.0052)
N	57853	57761	57761	54632
N cells	88	88	88	88
Panel B: Processing Capacity-weighted Events ( $w_{ip}$ varies by $i, p$ )				
$\beta$	0.25*** (0.074)	0.00071*** (0.00016)	5.23*** (1.78)	0.020* (0.011)
N	47861	28487	28487	27129
N cells	43	43	43	43

**Notes:** All regressions include cell-by-month and cell-by-year fixed effects. Column (1) is a fixed effects Poisson regression to account for many cells with zero flaring, whereas Columns (2) to (4) are standard panel regressions. Standard errors are clustered at the cell level. \*\*\* indicates significance at the 1% level, \*\* at the 5% level, \* at the 10% level.

## 4 Well-level analysis

In Section 3, we established that pipeline maintenance events affect pipeline capacity, and that changes in these have effects on flaring and methane emissions. Now, we focus on individual wells to study how flaring, production, and average netback prices respond to transmission line conditions.

Production data are self-reported to the Texas Railroad Commission (production and flaring) and the Texas Comptroller (value and volume of both liquids and gas sales) at a monthly level for gas wells and oil leases, which we refer to as “oil wells” in this section. We match each well in the Permian to the closest processing plant via gathering line distances. In our regression, we include only wells that are matched to one of the 66 plants that we can match to an interstate pipeline.<sup>26</sup>

As in the previous Section 3, we examine pipeline maintenance events that temporarily reduce capacity. Our estimating equation is

$$Y_{ikpt} = \alpha_0 + \alpha_1 \mathbb{1}_{kt} + \lambda_i + \gamma_t + \delta_{k,year(t)} + \rho_{p,month(t)} + \varepsilon_{ikpt} \quad (5)$$

where  $i$  indexes well,  $k$  indexes plant,  $p$  indexes subplay (Delaware, Central and Midland as shown in Figure 2), and  $t$  indexes month. The LHS variable  $Y_{ikpt}$  is our outcome of interest. The variable  $\mathbb{1}_{kt} \in [0, 1]$  is a continuous variable representing the proportion of month  $t$  there is an event on a pipeline connected to plant  $k$ . Here, a value of  $\mathbb{1}_{kt} = 0$  would represent no events on any day in the month, and a value of 1 would represent an event impacting every day of the month. We include well FE  $\lambda_i$ , time FE  $\gamma_t$ , seasonal subplay-month FE  $\rho_{p,month(t)}$  and plant-year FE  $\delta_{k,year(t)}$ . Identification stems from two assumptions. First, we assume that pipeline maintenance events are unrelated to individual wells’ short-term characteristics. Second, we assume that wells connected to processing plants on pipelines not undergoing maintenance events are representative of the counterfactual outcomes of impacted wells in a given month  $t$ .

### 4.1 Primary well-level analysis

Estimates of (5) are shown in Table 4 for four outcomes in panels A–D: levels of self-reported monthly flaring, gas production, oil production and average wellhead prices. Because revenues from gas are less important for oil versus gas-directed wells, we expect behavior might

---

<sup>26</sup>There are 208 operational plants in the full sample in our dataset. We connect 123 of them to at least one well but drop wells that were never observed flaring or producing during our time period. Plants that are not matched are those likely only connected to an intrastate pipeline.

Table 4: Primary Results: Impact of Pipeline Events on Well Activity

	Both		Oil leases		Gas wells	
	(1)	(2)	(3)	(4)	(5)	(6)
<b>Panel A: Flaring</b>						
<i>Event</i>	213.248** (85.695)	213.266** (85.695)	264.186*** (97.180)	264.189*** (97.187)	21.305 (183.465)	24.773 (183.321)
<i>Event · VI</i>		-956.812 (1081.285)		24.178 (234.481)		-2872.672 (2870.809)
<i>N</i>	590,133	590,133	409,498	409,498	180,629	180,629
adj. <i>R</i> <sup>2</sup>	0.314	0.314	0.270	0.270	0.385	0.385
<b>Panel B: Gas Production</b>						
<i>Event</i>	-1657.366*** (474.790)	-1657.167*** (474.788)	-581.641 (520.052)	-581.583 (520.063)	-4517.178*** (981.690)	-4476.281*** (980.559)
<i>Event · VI</i>		-10351.655 (9372.796)		418.599 (1443.921)		-33878.898 (25213.379)
<i>N</i>	590,133	590,133	409,498	409,498	180,629	180,629
adj. <i>R</i> <sup>2</sup>	0.782	0.782	0.771	0.771	0.796	0.796
<b>Panel C: Oil Production</b>						
<i>Event</i>	-177.732 (197.674)	-177.660 (197.674)	-200.558 (243.996)	-200.943 (244.004)	-536.049*** (150.022)	-528.402*** (149.796)
<i>Event · VI</i>		-3774.829*** (1303.721)		-2790.968*** (873.816)		-6334.394* (3294.626)
<i>N</i>	590,133	590,133	409,498	409,498	180,629	180,629
adj. <i>R</i> <sup>2</sup>	0.689	0.689	0.684	0.684	0.736	0.736
<b>Panel D: Log of Average Well Prices</b>						
<i>Event</i>	-0.038*** (0.012)	-0.038*** (0.012)	0.003 (0.012)	0.003 (0.012)	0.428*** (0.046)	0.433*** (0.046)
<i>Event · VI</i>		-0.697* (0.419)		0.246 (0.230)		-4.521** (2.235)
<i>N</i>	211,944	211,944	143,612	143,612	68,327	68,327
adj. <i>R</i> <sup>2</sup>	0.835	0.835	0.845	0.845	0.831	0.831
Well FE	Y	Y	Y	Y	Y	Y
Time FE	Y	Y	Y	Y	Y	Y
Plant-Year FE	Y	Y	Y	Y	Y	Y
Play-Month FE	Y	Y	Y	Y	Y	Y
<i>N</i> plants	66	64	55	66	64	55
<i>N</i> plant-groups	51	49	44	51	49	44

**Notes:** This table reports estimates the impact of a maintenance event for the interstate transmission line linked to the well via it's closest natural gas plant on reported well-level production, flaring, and average gas sale price using our baseline equation. Columns (1) and (2) consider all wells, columns (3) and (4) consider oil leases, and columns (5) and (6) consider gas wells. Columns (2), (4), and (6) expand our baseline equation to include the differential impact of vertical integration. We use one-way well-year-level clustered standard errors. \*\*\* indicates significance at the 1% level, \*\* at the 5% level, and \* at the 10% level.

**Sample:** Well-month level data from the TRCC beginning in December 2015 and ending in 2021. We only include 10,262 oil leases and 4,398 gas wells connected to a gas plant via gathering lines. Panel D restricts this sample to those wells with prices greater than the plant median in the previous month and whose average prices were between the bottom 1 and top 1 percentile. This corresponds to 6,670 oil wells and 3,222 gas wells.

differ between the two types. Given this, we separately estimate (5) for the three groups—an overall effect for *All wells*, an effect for *Oil wells* (leases), and an effect for *Gas wells*.

In general, coefficients in Table 4 have the expected signs and magnitudes. Column (1) of Panel A shows that following an increase in pipeline maintenance events, there is a statistically significant increase in average flaring across all connected wells. However, comparing columns (3) and (5) shows that the flaring response from oil wells is driving this increase, and there is no statistically or economically significant flaring response from gas wells.

We next examine the production responses from maintenance events. Panels B and C of Table 4 show that production from gas wells—be it gas or oil production—is much more responsive to maintenance events relative to oil wells. Unlike gas wells, oil wells do not exhibit statistically significant changes in production in response to a pipeline maintenance event. This is consistent with the idea that the value of associated gas is not the primary driver of production decisions for oil wells, particularly given that firms can flare gas when there are midstream constraints. In contrast, a much higher share of revenue at gas-directed wells comes from selling gas. These should be much more responsive to reductions in the available takeaway capacity. We interpret the observed responses to a decreases in pipeline capacity in the following way. Holding unused processing capacity is expensive for plant and well operators. Plant owners are likely to try to operate plants near their individual processing capacity, so maintenance events that limit the ability of processors to send gas on transmission should immediately reduce gas volumes. Similarly, operators are likely to complete wells to fit currently available capacity, rather than maintaining a stock of completed but non-producing wells that exceed the capacity of nearby processing.

Overall, these results help to reconcile the heterogeneous flaring responses observed in Panel A. Oil wells are more likely to continue producing oil and simply flare more gas when the system is constrained. In contrast, gas wells are more likely to reduce production so that they do not have to flare it, as gas production represents a larger share of these wells' revenues. We conjecture that gas wells may secure a higher proportion of firm transportation capacity rights on interstate pipelines, while oil wells would be more likely to use interruptible transportation capacity. We also note that the secondary capacity market is bilateral (Mohlin 2021) and may be subject to search frictions. Thus, when pipeline capacity is scarce, gas wells with firm transportation are more likely to be able to keep producing and capturing gas, but oil wells with only interruptible capacity rights may need to flare to continue producing.

Finally, we examine the responses of the log of average wellhead prices to changes in capacity (Panel D of Table 4). We calculate the average wellhead price as the value of the product sold divided by the volume, which is effectively a volume-weighted average of

daily wellhead prices. The challenge in examining these prices is that they are average, not marginal prices, and influenced by selection. When constraints arise, wells with unfavorable contracts and low prices will be less likely to appear in the price data. When they drop out, this is a form of extensive-margin selection that will bias our coefficient upward. Since the prices are volume-weighted averages, when wells that continue producing during a congestion period lower their quantity of gas sold, this congested price gets under-weighted, which is selection on an intensive margin. We attempt to correct for the extensive-margin selection bias by keeping only observations where prices in the previous period were above the median price for wells selling to the corresponding plant. We reason that contracts with processors are long-term agreements, so wells prices below the median in time  $t - 1$  will be most likely to experience low prices in  $t$  and will be more likely to drop out in response to transmission constraints. Our price data also include outliers—negative prices and prices in the many thousands of dollars, so we trim the top and bottom 1 percent, and any prices where reported volumes were negative.

Panel D of Table 4 shows that the log prices at oil wells do not respond to maintenance events, but log prices do rise at gas wells, potentially because of selection on the intensive margin (recall that Panel B, column (5) shows that these wells produce less during a congested month). When pooled, the effect is a small but statistically significant decrease in the log of average prices. We offer two explanations for this unintuitive finding. First, there is likely a disequilibrium when capacity is constrained where wellhead prices don't properly adjust to clear the market. Prices with processing plants are set through long-term contracts, and wells may hold differing types of capacity on the pipeline (firm vs interruptible). There are likely frictions that prevent efficient reallocation of capacity for short periods. Second, this may simply be a manifestation of Simpson's paradox where splitting the sample by lease type leads to imprecision in the estimation of the effect of these rare maintenance events separate from time effects (Simpson 1951). Regardless of the explanation, this analysis demonstrates that netback prices do decline overall during capacity constraints. We note that without limiting the sample to observations with above-median prices in the previous month, the effect is zero.

In our second well-level analysis, we test for whether vertically-integrated wells that share an operator with the plant respond differently to maintenance events compared to dis-integrated pairs of wells and plants. To do this, we re-estimate (5) and add an interaction between the event variable  $\mathbb{1}_{kt}$  and a well-plant indicator for whether the well and plant share a common operator.<sup>27</sup> Because we lack any (quasi)-exogenous variation in whether

---

<sup>27</sup>The sets of vertically integrated operators we can identify are from Anadarko, Conoco Phillips, Devon, Occidental, West Texas Gas, Chevron, and XTO.

wells and plants are vertically integrated, we cannot interpret these results in a causal sense. However, they do provide descriptive evidence for how market structure is correlated with firms' choices.

Results in columns (2), (4), and (6) of Table 4 show the differential responses by vertically integrated wells to maintenance events. Starting with Panel A, the results in columns (2), (4), and (6) indicate there is no statistically significant difference in the flaring responses of vertically integrated wells to maintenance events. However, the estimated differential effect is modestly negative for vertically integrated gas wells. This suggests that coordination in production and processing for vertically integrated wells does not have an economically meaningful impact on flaring when effective processing capacity declines, but this result is not conclusive for gas wells (p-value 0.31). In support of these findings, Panel B of Table 4 shows that the contemporaneous production response from vertically integrated wells—be it gas or oil—is statistically indistinguishable to the response to maintenance events by non-vertically integrated wells. In contrast, the panel D results in columns (2), (4), and (6) for changes in oil production following these maintenance events are statistically significant and of the expected sign. Overall, these results demonstrate that when a well and natural gas processing facility share the same operator there may be some coordination in terms of short term well-level production as a response to processing conditions, potentially due to contracts that give them priority with pipeline takeaway capacity, but this doesn't correspond with a statistically significant change in the level of flaring when capacity is constrained.

Panel D of Table 4 investigates whether the log of average netback price response to processing shocks is different for vertically integrated wells versus their non-integrated counterparts. Interestingly, we find that for the subset of vertically integrated wells there is a statistically significant decrease in the log of average netback price from maintenance events, particularly at gas wells. This suggests that vertically integrated wells may undertake contracts that substantially differ from other wells.

The primary takeaway from these well level analyses is that there is some heterogeneity in the well-level flaring response to changes in transmission capacity, and this has a few implications for policy. First, the results indicating that oil wells do not alter production in response to changes in transmission demonstrate the importance of having excess capacity available in oil-directed areas. Second, the suggestive price analysis and vertically integrated well analysis provide modest support for the potential inter-mediating role played by market structure in determining the effectiveness of gas processing infrastructure for reducing total flaring.

## 5 Conclusion

In this paper, we estimate the quantity of upstream flaring and methane emissions caused by congestion in midstream transmission infrastructure. We find that congestion has caused around 34 percent of upstream flaring and 10 percent of methane emissions. Over our sample period 2015–21, this led to annual climate costs of around \$1.2 billion. At the well-level, we find that oil wells—which produce more than half of the gas in the Texas Permian—choose to flare rather than scale back production when faced with transmission constraints. In contrast, gas wells reduce production to avoid flaring, reflecting their different incentives: gas wells’ revenues depend primarily on gas sales, while oil wells treat gas as a byproduct of oil production. Finally, we find suggestive evidence that vertically integrated producers exhibit a production response to transmission shocks, consistent with anecdotal evidence on the role of firm characteristics in flaring (Kilian 2020).

Our results contribute to the understanding of the systemic causes of flaring, how flaring coincides with methane emissions, and how market structure may play a role. This analysis is particularly relevant to current policy discussions in several ways. First, EPA has justified recent flaring restrictions on the basis of methane emitted from incomplete combustion (U.S. EPA 2024b). However, our estimates indicate that the climate costs for methane emissions and flaring emissions from midstream congestion are roughly comparable. This implies that the new federal price for methane emissions (the “Waste Emissions Charge” (WEC) underprices flaring relative to the optimal level because it ignores the CO<sub>2</sub> component (Appendix Table E.3). Second, new EPA prohibitions on flaring exempt flaring associated midstream congestion (U.S. EPA 2024b), even though our results indicate this likely excludes between 34% to 90% of flaring in the largest U.S. shale play studied, the Permian Basin. Given this under-regulation of flaring, alternative policies such as promotion of additional investment in midstream infrastructure could help reduce both flaring and methane emissions, though overbuilding of infrastructure also has economic costs.

Third, although our analysis focuses on the short run, our finding that oil production is not responsive to midstream capacity raises the possibility that they might not respond in the long run, either. This contrasts with the “fundamental law of road congestion,” which suggests that demand for transportation is perfectly elastic, so that increases in transportation capacity do not reduce congestion in the long run (Duranton and Turner 2011). If oil production is inelastic with respect to midstream gas capacity, promoting more capacity could lower climate costs from oil production. Alternatively, this result indicates that leasing minerals and generally promoting oil leases in areas with more available midstream infrastructure may lead to lower climate costs from oil production. Additional results from our

well-level analysis indicate that market structure also matters for understanding the effectiveness of additional midstream infrastructure. Given that we focus specifically on short-run, however, further study is needed to understand the long-term relationships between supply of midstream capacity, oil production, and emissions.

Outside of providing several policy insights, our study differs in important ways from the emerging literature on transportation infrastructure and environmental impacts from energy production. Specifically, for electricity markets, transportation constraints can shift the location, quantity, and external costs of emissions (Fell et al. 2021). In oil and gas producing regions, by contrast, we find that gas is inelastically produced as a by-product of oil as a result of past decisions to complete a well. When transportation capacity becomes constrained, we show that oil producers change from viewing the gas as a valuable commodity to disposing of it as a by-product through flaring or venting and creating an environmental externality. Flaring and methane emissions from associated gas are examples of the challenges involved in optimizing a transportation network for multiple scales, environmental externalities, and joint production of resources. This type of problem is likely to be important in many contexts associated with the energy transition. Biogas from waste streams (Hengeveld et al. 2016; Hoo et al. 2018; Shen et al. 2015), lithium production from brine at geothermal energy sites (Finster et al. 2015; Schenker et al. 2024), and cobalt from copper and gold mines (Jordan 2018; Jordan 2017) are all examples where externalities may be determined by how supply chains are scaled to accommodate joint production.

A related literature examines how transportation constraints create local market power for sellers within network nodes, with sellers sometimes manipulating these constraints to generate rents (Borenstein et al. 2000; Hausman 2024; Woerman 2019). Although our setting differs, we similarly document significant social costs from transmission constraints and evidence that market structure matters. Our results may be explained by vertically integrated oligopolistic midstream firms constraining processing capacity to generate rents (Salop and Scheffman 1983). Alternatively, our findings could be attributable congestion shocks entailing coordination costs more easily handled within vertically integrated firms. We caution that our market structure results are conditional correlations and identifying what drives the differential responses to congestion—through market power, contracts, or physical constraints—is a topic for future research.

Several directions for future research emerge from our analysis. First, understanding how contract structure and capacity prioritization in the gathering system influence our results could be valuable. Second, while we have quantified the contribution of limited transmission capacity to flaring, examining the effects of gathering and processing capacity on local flaring levels could also be important. Third, spatial measures of midstream competition deserve at-

tention, such as how competition in gas processing affects flaring by wells. Finally, repeating our analysis with more detailed methane emissions data would be valuable—computational limitations prevented us from conducting more detailed inversions that map methane concentrations to emissions at a fine grid scale. Future work could better identify methane emissions from wells, processing facilities, and transmission infrastructure, providing deeper insight into emissions across the natural gas supply chain.

## References

- Agerton, Mark, Ben Gilbert, and Gregory B. Upton (2023). “The Economics of Natural Gas Flaring and Methane Emissions in US Shale: An Agenda for Research and Policy”. *Review of Environmental Economics and Policy* 17.2, 251–273. DOI: [10.1086/725004](https://doi.org/10.1086/725004).
- Agerton, Mark and Gregory B. Upton Jr. (2019). “Decomposing Crude Price Differentials: Domestic Shipping Constraints or the Crude Oil Export Ban?” *The Energy Journal* 40.3. DOI: [10.5547/01956574.40.3.mage](https://doi.org/10.5547/01956574.40.3.mage).
- Allen, David T, Adam P Pacsi, David W Sullivan, et al. (2015). “Methane emissions from process equipment at natural gas production sites in the United States: Pneumatic controllers”. *Environmental science & technology* 49.1, 633–640.
- Beatty, Lauren (2022). “How Do Natural Gas Pipeline Networks Affect Emissions From Drilling and Flaring?” Job market paper.
- Black, Katie Jo, Andrew J Boslett, Elaine L Hill, Lala Ma, and Shawn J McCoy (2021). “Economic, environmental, and health impacts of the fracking boom”. *Annual Review of Resource Economics* 13, 311–334.
- Blundell, Wesley and Anatolii Kokoza (2022). “Natural Gas Flaring, Respiratory Health, and Distributional Effects”. *Journal of Public Economics* 208, 104601. DOI: [10.1016/j.jpubeco.2022.104601](https://doi.org/10.1016/j.jpubeco.2022.104601).
- Borenstein, Severin, James Bushnell, and Steven Stoff (2000). “The Competitive Effects of Transmission Capacity in a Deregulated Electricity Industry”. *The RAND Journal of Economics* 31.2, 294–325. DOI: [10.2307/2601042](https://doi.org/10.2307/2601042).
- Boslett, Andrew, Elaine Hill, Lala Ma, and Lujia Zhang (2021). “Rural Light Pollution from Shale Gas Development and Associated Sleep and Subjective Well-Being”. *Resource and Energy Economics* 64, 101220. DOI: [10.1016/j.reseneeco.2021.101220](https://doi.org/10.1016/j.reseneeco.2021.101220).
- Brantley, Halley L, Eben D Thoma, William C Squier, Birnur B Guven, and David Lyon (2014). “Assessment of methane emissions from oil and gas production pads using mobile measurements”. *Environmental science & technology* 48.24, 14508–14515.
- Clay, Karen, Akshaya Jha, Nicholas Muller, and Randall Walsh (2017). *The External Costs of Transporting Petroleum Products by Pipelines and Rail: Evidence From Shipments of Crude Oil from North Dakota*. Working Paper 23852. National Bureau of Economic Research. DOI: [10.3386/w23852](https://doi.org/10.3386/w23852).
- Covert, Thomas, Ludovica Gazze, Michael Greenstone, and Olga Rostapshova (2024). “Using Remote Sensing to Track and Regulate Oil and Gas Methane Emissions in Colorado”.
- Covert, Thomas R and Ryan Kellogg (2017). *Crude by Rail, Option Value, and Pipeline Investment*. Working Paper 23855. National Bureau of Economic Research. DOI: [10.3386/w23855](https://doi.org/10.3386/w23855).
- Cremer, Helmuth and Jean-Jacques Laffont (2002). “Competition in Gas Markets”. *European Economic Review* 46.4, 928–935. DOI: [10.1016/S0014-2921\(01\)00226-4](https://doi.org/10.1016/S0014-2921(01)00226-4).
- Dunkle Werner, Karl and Wenfeng Qiu (2024). “Information Matters: Feasible Policies for Reducing Methane Emissions”. *Journal of the Association of Environmental and Resource Economists*.
- Duranton, Gilles and Matthew A Turner (2011). “The fundamental law of road congestion: Evidence from US cities”. *American Economic Review* 101.6, 2616–2652.

- EDF (2021). *PermianMAP Final Report: A Look Back at Key Findings and Takeaways from the Permian Methane Analysis Project*. Environmental Defense Fund.
- Elvidge, Christopher D., Mikhail Zhizhin, Kimberly Baugh, Feng-Chi Hsu, and Tilottama Ghosh (2016). “Methods for Global Survey of Natural Gas Flaring from Visible Infrared Imaging Radiometer Suite Data”. *Energies* 9.1 (1), 14. DOI: [10.3390/en9010014](https://doi.org/10.3390/en9010014).
- Elvidge, Christopher D., Mikhail Zhizhin, Feng-Chi Hsu, and Kimberly E. Baugh (2013). “VIIRS Nightfire: Satellite Pyrometry at Night”. *Remote Sensing* 5.9 (9), 4423–4449. DOI: [10.3390/rs5094423](https://doi.org/10.3390/rs5094423).
- Federal Reserve Bank of Dallas (2019). *Dallas Fed Energy Survey*. Fourth Quarter 2019.
- (2024). *Dallas Fed Energy Survey*. Second Quarter 2024.
- Fell, Harrison, Daniel T. Kaffine, and Kevin Novan (2021). “Emissions, Transmission, and the Environmental Value of Renewable Energy”. *American Economic Journal: Economic Policy* 13.2, 241–272. DOI: [10.1257/pol.20190258](https://doi.org/10.1257/pol.20190258).
- Finster, Molly, Corrie Clark, Jenna Schroeder, and Louis Martino (2015). “Geothermal produced fluids: Characteristics, treatment technologies, and management options”. *Renewable and Sustainable Energy Reviews* 50, 952–966.
- Fitzgerald, Timothy and Case Stiglbauer (2015). “Flaring of Associated Natural Gas in the Bakken Shale”.
- Hausman, Catherine (2024). *Power Flows: Transmission Lines, Allocative Efficiency, and Corporate Profits*. DOI: [10.3386/w32091](https://doi.org/10.3386/w32091). Pre-published.
- Hausman, Catherine and Lucija Muehlenbachs (2018). “Price Regulation and Environmental Externalities: Evidence from Methane Leaks”. *Journal of the Association of Environmental and Resource Economists* 6.1, 73–109. DOI: [10.1086/700301](https://doi.org/10.1086/700301).
- Hengeveld, Evert Jan, Jan Bekkering, WJT Van Gemert, and AA Broekhuis (2016). “Biogas infrastructures from farm to regional scale, prospects of biogas transport grids”. *Biomass and Bioenergy* 86, 43–52.
- Hoo, Poh Ying, Haslenda Hashim, and Wai Shin Ho (2018). “Opportunities and challenges: Landfill gas to biomethane injection into natural gas distribution grid through pipeline”. *Journal of Cleaner Production* 175, 409–419.
- Howard, Touché, Thomas W. Ferrara, and Amy Townsend-Small (2015). “Sensor Transition Failure in the High Flow Sampler: Implications for Methane Emission Inventories of Natural Gas Infrastructure”. *Journal of the Air & Waste Management Association* 65.7, 856–862. DOI: [10.1080/10962247.2015.1025925](https://doi.org/10.1080/10962247.2015.1025925).
- Hu, Haili, Otto Hasekamp, André Butz, et al. (2016). “The Operational Methane Retrieval Algorithm for TROPOMI”. *Atmospheric Measurement Techniques* 9.11, 5423–5440. DOI: [10.5194/amt-9-5423-2016](https://doi.org/10.5194/amt-9-5423-2016).
- Hu, Haili, Jochen Landgraf, Rob Detmers, et al. (2018). “Toward Global Mapping of Methane With TROPOMI: First Results and Intersatellite Comparison to GOSAT”. *Geophysical Research Letters* 45.8, 3682–3689. DOI: [10.1002/2018GL077259](https://doi.org/10.1002/2018GL077259).
- IAWG (2021). *Social Cost of Carbon, Methane, and Nitrous Oxide Interim Estimates under Executive Order 13990*. Technical Support Document. Interagency Working Group on Social Cost of Greenhouse Gases, 48.
- IEA (2023a). *Emissions from Oil and Gas Operations in Net Zero Transitions: A World Energy Outlook Special Report on the Oil and Gas Industry and COP28*. doi:<https://doi.org/10.1787/317cb1en>. Paris: OECD Publishing.

- IEA (2023b). *Tracking Clean Energy Progress 2023*.
- Jordan, Brett (2018). “Economics literature on joint production of minerals: A survey”. *Resources Policy* 55, 20–28.
- Jordan, Brett W (2017). “Companions and competitors: Joint metal-supply relationships in gold, silver, copper, lead and zinc mines”. *Resource and Energy Economics* 49, 233–250.
- Kilian, Lutz (2020). *What Is the U.S. oil industry doing about greenhouse gas emissions?* Federal Reserve Bank of Dallas. URL: <https://www.dallasfed.org/research/economics/2020/1229>.
- Lade, Gabriel E. and Ivan Rudik (2020). “Costs of Inefficient Regulation: Evidence from the Bakken”. *Journal of Environmental Economics and Management* 102, 102336. DOI: [10.1016/j.jeem.2020.102336](https://doi.org/10.1016/j.jeem.2020.102336).
- LaRiviere, Jacob and Xueying Lyu (2022). “Transmission Constraints, Intermittent Renewables and Welfare”. *Journal of Environmental Economics and Management* 112, 102618. DOI: [10.1016/j.jeem.2022.102618](https://doi.org/10.1016/j.jeem.2022.102618).
- Lau, Peiley (2020). “The Extraordinary Rise of Unreported Gas Flaring Among Fracking Firms”.
- Lin, Wei and Jeffrey M Wooldridge (2019). “Testing and correcting for endogeneity in non-linear unobserved effects models”. In: *Panel data econometrics*. Elsevier, 21–43.
- Lyon, David R, Benjamin Hmiel, Ritesh Gautam, et al. (2021). “Concurrent variation in oil and gas methane emissions and oil price during the COVID-19 pandemic”. *Atmospheric Chemistry and Physics* 21.9, 6605–6626.
- Mitchell, Austin L., Daniel S. Tkacik, Joseph R. Roscioli, et al. (2015). “Measurements of Methane Emissions from Natural Gas Gathering Facilities and Processing Plants: Measurement Results”. *Environmental Science & Technology* 49.5, 3219–3227. DOI: [10.1021/es5052809](https://doi.org/10.1021/es5052809).
- Mohlin, Kristina (2021). “The U.S. Gas Pipeline Transportation Market: An Introductory Guide with Research Questions for the Energy Transition”. *SSRN Electronic Journal*. DOI: [10.2139/ssrn.3775725](https://doi.org/10.2139/ssrn.3775725).
- Oliver, Matthew E., Charles F. Mason, and David Finnoff (2014). “Pipeline Congestion and Basis Differentials”. *Journal of Regulatory Economics* 46.3, 261–291. DOI: [10.1007/s11149-014-9256-9](https://doi.org/10.1007/s11149-014-9256-9).
- Plant, Genevieve, Eric A. Kort, Adam R. Brandt, et al. (2022). “Inefficient and Unlit Natural Gas Flares Both Emit Large Quantities of Methane”. *Science* 377.6614, 1566–1571. DOI: [10.1126/science.abq0385](https://doi.org/10.1126/science.abq0385).
- Preonas, Louis (2019). “Market Power in Coal Shipping and Implications for U.S. Climate Policy”. Working Paper.
- Salop, Steven C and David T Scheffman (1983). “Raising rivals’ costs”. *The American economic review* 73.2, 267–271.
- Schenker, Vanessa, Peter Bayer, Christopher Oberschelp, and Stephan Pfister (2024). “Is lithium from geothermal brines the sustainable solution for Li-ion batteries?” *Renewable and Sustainable Energy Reviews* 199, 114456.
- Shen, Yanwen, Jessica L Linville, Meltem Urgun-Demirtas, Marianne M Mintz, and Seth W Snyder (2015). “An overview of biogas production and utilization at full-scale wastewater treatment plants (WWTPs) in the United States: challenges and opportunities towards energy-neutral WWTPs”. *Renewable and Sustainable Energy Reviews* 50, 346–362.

- Simpson, Edward H (1951). “The interpretation of interaction in contingency tables”. *Journal of the Royal Statistical Society: Series B (Methodological)* 13.2, 238–241.
- Stranlund, John K and Insung Son (2019). “Prices versus Quantities versus Hybrids in the Presence of Co-pollutants”. *Environmental and resource economics* 73, 353–384.
- Thu, Wint Myat (2023). “Relieving Midstream Constraints in Natural Gas Flaring”. Job market paper.
- Tran, Huy, Erin Polka, Jonathan J. Buonocore, et al. (2024). “Air Quality and Health Impacts of Onshore Oil and Gas Flaring and Venting Activities Estimated Using Refined Satellite-Based Emissions”. *GeoHealth* 8.3, e2023GH000938. DOI: [10.1029/2023GH000938](https://doi.org/10.1029/2023GH000938).
- U.S. EPA (2023). *EPA Report on the Social Cost of Greenhouse Gases: Estimates Incorporating Recent Scientific Advances*. Docket ID No. EPA-HQ-OAR-2021-0317. U.S. Environmental Protection Agency.
- (2024a). “Greenhouse Gas Reporting Rule: Revisions and Confidentiality Determinations for Petroleum and Natural Gas Systems”. *Fed. Reg.* 89, 42062–42327.
- (2024b). “Standards of Performance for New, Reconstructed, and Modified Sources and Emissions Guidelines for Existing Sources: Oil and Natural Gas Sector Climate Review”. *Fed. Reg.* 89, 16820–17227.
- (2024c). “Waste Emissions Charge for Petroleum and Natural Gas Systems”. *Fed. Reg.* 89, 5318–5381.
- Varon, Daniel J., Daniel J. Jacob, Benjamin Hmiel, et al. (2023). “Continuous Weekly Monitoring of Methane Emissions from the Permian Basin by Inversion of TROPOMI Satellite Observations”. *Atmospheric Chemistry and Physics* 23.13, 7503–7520. DOI: [10.5194/acp-23-7503-2023](https://doi.org/10.5194/acp-23-7503-2023).
- Woerman, Matt (2019). “Market Size and Market Power: Evidence from the Texas Electricity Market”. Job market paper.
- Zavala-Araiza, Daniel, Ramón A. Alvarez, David R. Lyon, et al. (2017). “Super-Emitters in Natural Gas Infrastructure Are Caused by Abnormal Process Conditions”. *Nature Communications* 8.1 (1), 1–10. DOI: [10.1038/ncomms14012](https://doi.org/10.1038/ncomms14012).
- Zavala-Araiza, Daniel, David Lyon, Ramón A. Alvarez, et al. (2015). “Toward a Functional Definition of Methane Super-Emitters: Application to Natural Gas Production Sites”. *Environmental Science & Technology* 49.13, 8167–8174. DOI: [10.1021/acs.est.5b00133](https://doi.org/10.1021/acs.est.5b00133).
- Zirogiannis, Nikolaos, Daniel H Simon, and Alex J Hollingsworth (2020). “Estimating co-pollutant benefits from climate change policies in the electricity sector: A regression approach”. *Energy Economics* 90, 104863.

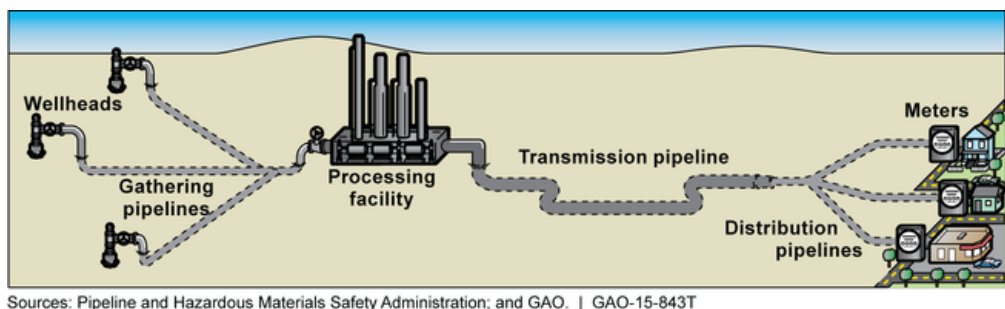


Figure A.1: Diagram of midstream segment

## A Online Appendix: Industry Overview

Agerton et al. (2023) provide a recent review of the literature on upstream flaring and methane emission, as well as an overview of the relevant segments of oil and gas value chain. Here, we provide a brief overview of relevant segments for this particular research.

Once produced, oil and gas must be transported from the well to market via the midstream segment. While oil can be transported by many modes within the U.S.—truck, rail, ship, or pipeline—in general, it is only economic to transport natural gas via pipeline.<sup>28</sup> Figure A.1 is a diagram of the midstream. As the diagram shows, the midstream segment is actually a suite of services and infrastructure. Once gas is extracted at the well, it is transported through a network of smaller gathering pipelines. Associated gas (gas produced alongside oil) generally contains more valuable, heavier hydrocarbons (ethane, butane, propane, etc) and other impurities alongside methane. Gas processing strips out these components: the waste is disposed, and high-value products are separated out for sale at higher prices. After being processed to pipeline specification, natural gas is moved to market via long-haul transmission pipelines.

Midstream services are rarely provided within the same upstream producing firm. Instead, midstream assets are typically owned and operated by midstream firms. Gathering and processing services in particular are usually procured through private, bilateral agreements, while transmission has a different market structure. For gathering, upstream firms generally sign a private, bilateral, long-term *acreage dedication* agreement. Under an acreage, dedication, a gathering company is designated as the exclusive gatherer for a certain area. It builds and operates the gathering system. The producer pays a volumetric charge for moving the gas via the system. Natural gas processing can be owned by the same company that owns the gathering, or by a different company.<sup>29</sup>

<sup>28</sup>It is also possible to super-cool natural gas until it becomes liquid at around  $-260^{\circ}\text{F}$  ( $-162^{\circ}\text{C}$ ), and then transport it via truck or ship. Such gas is referred to as “liquefied natural gas” or “LNG.” Liquefaction, however, is generally both capital and energy-intensive. While small-scale LNG liquefaction plants exist, liquefaction is most economical at scale. Thus, LNG is generally associated with transporting gas in large, seaborne cargoes when pipelines are impractical.

<sup>29</sup>There are three typical pricing structures for gas processing. A *fee* basis involves a set price per unit of gas. *Percent of proceeds* allows processors to keep part of the revenues from sale of both the lower-valued natural gas (methane) and its higher-valued NGL components. *Keep whole* pricing allows the processor to extract and sell high-value NGLs and return an equivalent volume of lower-value methane to the producers (Followill et al. 2008; Kafka and Strawn 2017). Commodity prices for NGLs and natural gas (methane) have

Rights to interstate transmission capacity can be purchased during the initial “open season” when the pipeline is constructed, or later on a secondary market. Prices are public, and they are determined under a few different frameworks established by FERC (American Gas Association 2007). FERC pricing regulations limit the ability of interstate transmission to charge rents as a natural monopoly. Transmission capacity comes in two main tiers: more expensive *firm* capacity—a guaranteed right to ship a particular volume except under exceptional circumstances or *force majeure*—or less expensive *interruptible* capacity—which can be denied if the pipeline is full. Different upstream producers can hold different amounts of firm versus interruptible capacity rights on the pipeline relative to their production. This means that different producers can be affected differently by congestion that limits the amount of capacity available to holders of interruptible capacity rights. Capacity rights are traded bilaterally in a secondary market (Mohlin 2021). We conjecture that gas wells are more likely to hold firm transportation rights on transmission lines because most of the profits from these wells are dependent on the ability to get gas to market, and oil wells are more likely to hold interruptible capacity rights.

## B Online Appendix: Data Construction

### B.1 Matching wells to processing plants

To match wells to pipelines, we first transformed the gathering pipeline shapefiles into a network and measured the distance along the gathering network from each well to all processing plants. Then, we matched each well to the plant that is closest in terms of distance along the gathering network. Matching processing plants to interstate pipelines was the second step. We purchased two separate datasets on processing plants from Wood Mackenzie. The first includes the physical locations, capacities, and expansions of 208 operational processing plants in the Permian. The second includes a subset of 50 plants, which are aggregated into 27 groups that are linked to nomination points on the four interstate pipelines. Grouped plants share a common operator and are generally located near one another. We group the remaining 158 plants into 115 groups based on name and physical proximity. Then we match these to interstate nomination points using a combination of plant and nomination point names (and historical names), operator and owner information in both datasets, physical proximity, and nomination point classifications by the pipeline. In total, we are able to match 53 of these plant-groups representing 73 plants to nomination points on our four interstate pipelines. Some of our matched plants are likely to be connected to both inter- and intrastate pipelines, but congestion on interstate pipelines will still affect them. Figure 3b shows the operational processing facilities in our dataset in addition to the set of transmission pipelines in Texas (inter and intrastate). We differentiate plants by how the plants were matched to interstate pipelines.

---

diverged at times, meaning that different upstream producers—even if they have the same bargaining power with the processing plant—have paid very different prices for gas processing.

## B.2 Construction of methane emissions

Most methane inversion models in the atmospheric science literature reduce to a linear relationship between observed concentration and unobserved emissions based on the following approach.<sup>30</sup> First, define some “background” level of ambient concentration that is assumed to be driven by natural processes. In the scientific literature this may be done through state-space modeling, secondary data, or averages of subsamples. We take the mean concentration in the Permian over the first four months of our sample as the background rate, under the assumption that most increases over the next several years are likely driven by increased oil and gas activity, which is the dominant change in land use in the Permian basin over this period. Next, the literature defines a methane “enhancement” as non-negative differences between detected and background concentration. Emissions are then calculated as a linear function of the enhancement, under the logic that elevated concentrations above the natural background must be due to emissions. In the scientific literature, the parameters of the linear relationship are determined by computational atmospheric chemistry and transport modeling. In our rough approximation, we rely on the linearity of the emissions-to-enhancement relationship to simply scale our calculated enhancement to roughly match levels of emissions reported in the scientific literature over the sample period.

## C Online Appendix: Theoretical model

**Overview** We write and solve a model of demand for pipeline capacity, which is split between firm and interruptible capacity rights. Firms are endowed with capacity rights, but can freely trade them. The main idea is that when capacity is constrained, interruptible transportation functions as a lottery, where winners can avoid the cost of purchasing firm capacity but still sell at the higher national price. Some losers of the lottery can still sell at the lower, local price, but some cannot and must flare. In equilibrium, the value of entering the lottery, purchasing firm capacity, or selling locally must be the same. The possibility of the lottery and the fact that some firms flare introduces a source of inefficiency to the model. Unlike a standard framework without frictions (Cremer and Laffont 2002), the lottery means that prices in the local market respond positively to national demand shocks when the pipeline is constrained. In a more standard framework, the basis differential (shadow value of pipeline capacity) absorbs the entirety of the national demand shock. In our model, flaring can increase when national demand increases because higher national prices make the lottery more valuable. Our model is also able to replicate the empirical fact that exogenous drops in pipeline capacity increase flaring and decrease local prices.

**Model details** The model is static. There is a pipeline with capacity  $K$  that connects the producing region to the national market  $N$ . Demand in the national market is perfectly elastic, and the national price is  $p_N$ . There is also a local market  $M$  with elastic demand

---

<sup>30</sup>See, for example, Barkley et al. (2022), Cusworth et al. (2022), Sheng et al. (2018), and Varon et al. (2023). Many of these models also implement a linear Bayesian filter in which a prior emissions estimate is taken from a secondary data source such as an inventory estimate, in-situ monitor, or flyover. The prior is then updated to a posterior emissions estimate using TROPOMI concentration data. In these cases, however, the underlying relationship is still linear.

and inverse demand  $D(p_M) = q_M$ . Producers are each endowed with one unit of natural gas. There is a mass  $\alpha$  of type  $F$  producers endowed with firm transport (FT) on the pipeline. FT guarantees they can sell gas directly to  $N$  at  $p_N$  as long as  $K$  exceeds production by type  $F$  firms,  $q_F$ . There is also a mass  $\beta$  of type  $I$  producers with interruptible capacity. Production costs are distributed identically between groups with distribution  $\theta \sim G(\cdot)$ .

We assume that not all pipeline capacity is sold as FT, e.g.,  $\alpha < K$ , and that the remainder is sold as interruptible transportation (IT) capacity. We also assume that gas supply can exceed pipeline capacity so that  $K < \alpha + \beta$ . FT may be traded freely at price  $\lambda$  in a secondary market. In the analysis below, we focus on the case when pipeline capacity is constrained because in a world where pipeline capacity is unconstrained,  $p_N = p_M$ , and no congestion-driven flaring occurs.

Our assumption that pipeline capacity exceeds FT rights ( $\alpha < K$ ) is an abstraction. In reality, pipelines may sell their entire capacity as FT (Oliver et al. 2014). However, federal regulations also require pipelines to also offer interruptible transportation (IT) service, which can take advantage of unused FT capacity rights (18 CFR 284.9). Even during congested times, it is reasonable to think that not all FT rights are used. FT capacity is transacted in bilateral exchanges (Mohlin 2021), which raises the likelihood of search frictions preventing some sales. Some firms with FT—say, local distribution companies, may also fail to use all of their FT capacity if demand is less than their FT rights. In another, more complicated version of this model, we assumed all pipeline capacity is sold as FT, but could only be traded via bilateral exchange in a decentralized market characterized by search frictions. In that version of the model, not all FT is utilized so that an IT lottery is still present.

Figure C.1 shows a decision tree for the model, with final payoffs in shaded gray boxes. The profit-maximization problem for a type- $F$  firm in a constrained environment is

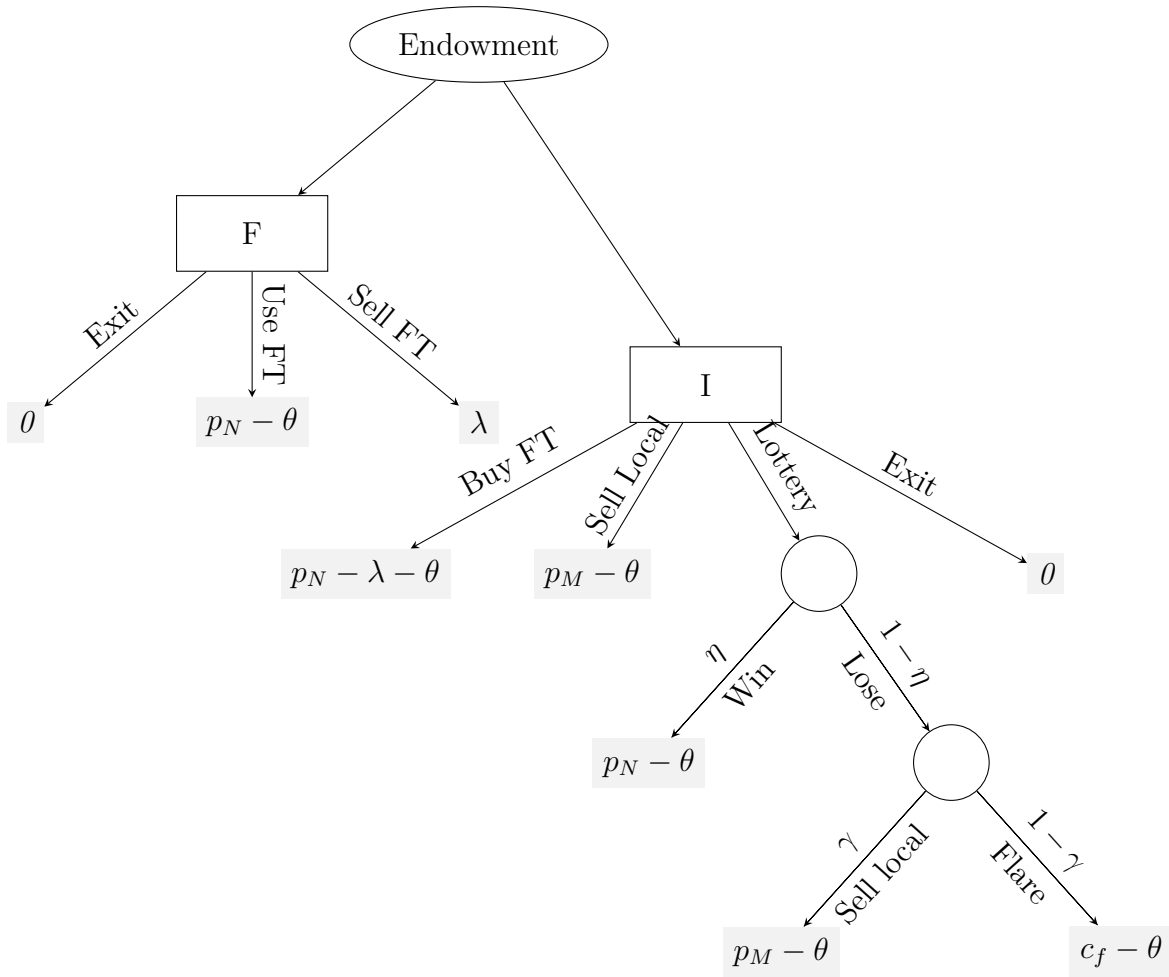
$$V^F(\theta) = \max \left\{ \underbrace{p_N - \theta}_{\text{Use FT}}, \underbrace{p_M - \theta}_{\text{Sell local}}, \underbrace{0}_{\text{exit}}, \underbrace{\lambda}_{\text{Sell FT}} \right\}.$$

In a constrained world none of the  $F$  firms exit, and all  $\alpha$  units of FT are used. Some type- $F$  firms produce at cost  $\theta$  and sell in the national market at price  $p_N$ . Type  $\theta^F = p_N - \lambda$  is the highest-cost type do so. Thus,  $q_{FN} = \alpha G(p_N - \lambda)$  ship to national market  $N$ , and  $q_{FI} = \alpha[1 - G(p_N - \lambda)]$  sell FT to  $I$ . Since  $p_N > p_M$ , no  $F$  firms ever sell locally.

Type  $I$  firms with only interruptible capacity have four options. Some ( $q_{IM}$ ) can choose to sell directly to local market  $M$ . Some ( $q_{IF}$ ) can choose to purchase FT from  $F$ . Some can exit  $q_{IO}$ , and some ( $q_{II}$ ) can try entering the interruptible lottery  $I$  to ship to  $N$ . If they try to use interruptible capacity  $I$ , with probability  $\eta$ ,  $q_{IIN} = q_{II}\eta$  are able to get on the pipeline and sell at  $p_N$ . With probability  $(1 - \eta)\gamma$ ,  $q_{IIM} = q_{II}(1 - \eta)\gamma$  can sell into  $M$  at price  $p_M$ , but with probability  $(1 - \eta)(1 - \gamma)$ ,  $q_{IIf} = q_{II}(1 - \eta)(1 - \gamma)$  are unable to and must flare with payoff  $c_f \in \mathbb{R}$ . The problem for type- $I$  firms is

$$V^I(\theta) = \max \left\{ \underbrace{\eta p_N}_{\text{on pipe}} + \underbrace{(1 - \eta)(1 - \gamma)c_f}_{\text{flare}} + \underbrace{(1 - \eta)\gamma p_M - \theta}_{\text{local sale}}, \underbrace{p_M - \theta}_{\text{local directly}}, \underbrace{0}_{\text{exit}}, \underbrace{p_N - \lambda}_{\text{buy FT}} \right\}$$

Figure C.1: Decision tree with final payoffs. Shaded boxes display final payoffs. Chance nodes are circles, with probabilities given along edges. Decision nodes are rectangles



Equilibrium requires indifference for types  $I$ , so that

$$p_M = p_N - \lambda \quad (6)$$

$$p_M = \eta p_N + (1 - \eta)(1 - \gamma)c_f + (1 - \eta)\gamma p_M. \quad (7)$$

Because types  $F$  and  $I$  can trade frictionlessly, marginal cost of production is the same across groups:  $\theta^F = \theta^I = p_M$ . This feature of the equilibrium is shared with the social planner's solution. However, the equilibrium departs from efficiency because too many  $I$  firms compete in the interruptible lottery, are unable to get space on the pipeline, and must flare (waste) their gas.

The supply from type- $I$  firms is split between firms that attempt the interruptible lottery  $I$ , those that sell directly to the local market  $M$ , and those that purchase FT from  $F$ :

$$q_I = q_{II} + q_{IM} + q_{IF}$$

We know that total supply is  $q_I = \beta G(p_M)$  because  $\theta^I = p_M$  is the threshold for exiting. In a constrained world, all of the  $\alpha$  FT permits are used first, so the number of firms who attempt the interruptible lottery and make it to  $N$  are  $q_{IIN} = K - \alpha$ . Thus,  $q_{II} = (K - \alpha)/\eta$ . Finally, we know that the local market demand is met by the firms that enter the interruptible lottery but go to  $M$  and those that directly go to  $M$ :  $q_M = q_{IIM} + q_{IM}$ , which implies that  $q_{IM} = q_M - q_{IIM}$ . Market clearing requires that  $q_M = D_M^{-1}(p_M)$ , and  $q_{IIM} = (1 - \eta)\gamma(K - \alpha)/\eta$ . We then put these equations together and use the indifference condition (6) to obtain:

$$\beta G(p_M) = \frac{K - \alpha}{\eta} + D_M^{-1}(p_M) - \frac{K - \alpha}{\eta}(1 - \eta)\gamma + \alpha[1 - G(p_M)]$$

Rearrange this equation, and (7) to obtain a vector valued equation  $f(y)$  where  $y = [p_M, \eta]$  and  $x$  contains exogenous parameters that characterizes the equilibrium:

$$f(y, x) = \left[ \begin{array}{c} \eta p_N + (1 - \eta)(1 - \gamma)c_f - [1 - (1 - \eta)\gamma]p_M \\ \frac{K - \alpha}{\eta} + D_M^{-1}(p_M) - \frac{K - \alpha}{\eta}(1 - \eta)\gamma + \alpha[1 - G(p_M)] - \beta G(p_M) \end{array} \right] := 0. \quad (8)$$

We are particularly interested in how  $y$  is affected by the national price, pipeline capacity, and the payoff to flaring:  $x = [p_N, K, c_f]$ . We approach this using the implicit function theorem, which implies that  $dy/dx = -J_y^{-1}J_x$  where  $J_z$  is the Jacobian of  $f$  with respect to

z. Note that  $J_y^{-1} = \frac{1}{\det(J_y)} \text{adj}(J_y)$  where  $\text{adj}(A)$  is the adjugate of matrix  $A$ .

$$\begin{aligned}
J_y &= \begin{bmatrix} -[1 - \gamma(1 - \eta)] & p_N - c_f(1 - \gamma) - p_M\gamma \\ (D^{-1})' - G'(\alpha + \beta) & -(K - \alpha)(1 - \gamma)\eta^{-2} \end{bmatrix} \\
\text{adj}(J_y) &= \begin{bmatrix} -(K - \alpha)(1 - \gamma)\eta_s^{-2} & -[(p_N - c_f)(1 - \gamma) + (p_N - p_M)\gamma] \\ (\alpha + \beta)G' - (D^{-1})' & -[1 - \gamma(1 - \eta)] \end{bmatrix} \\
\det(J_y) &= (K - \alpha)(1 - \gamma)[1 - \gamma(1 - \eta)]\eta^{-2} \\
&\quad + [(p_N - c_f)(1 - \gamma) + (p_N - p_M)\gamma][(\alpha + \beta)G' - D'] \\
J_x &= \begin{bmatrix} \eta & 0 & (1 - \gamma)(1 - \eta) \\ 0 & [1 - \gamma(1 - \eta)]\eta^{-1} & 0 \end{bmatrix}
\end{aligned}$$

The determinant  $\det(J_y)$  is positive. It is straightforward to sign  $\text{adj}(J_y)$  (since demand is downward-sloping  $((D^{-1})' < 0)$ , and therefore also  $J_y^{-1}$ .  $J_x$  is also easy to sign:

$$\det(J_y) : + \qquad J_y^{-1} : \begin{bmatrix} - & - \\ + & - \end{bmatrix} \qquad J_x : \begin{bmatrix} + & 0 & + \\ 0 & + & 0 \end{bmatrix}.$$

This implies that we can sign how changes in  $x_j$  affect equilibrium value  $y_i$ :

$$\frac{dy}{dx} = \frac{dp_M}{d\eta} \begin{pmatrix} dp_N & dK & dc_f \\ + & + & + \\ - & + & - \end{pmatrix}$$

A key object for us is the quantity of flaring, and how it responds to exogenous shocks:

$$q_{IIfl} = \frac{K - \alpha}{\eta}(1 - \eta)(1 - \gamma).$$

When the probability of getting on the pipeline rises, flaring goes down:

$$\frac{\partial q_{IIfl}}{\partial \eta} = -(K - \alpha)(1 - \gamma)\eta^{-2} < 0,$$

so factors that raise  $\eta$  reduce flaring. This, in turn, implies that *in a constrained environment*, flaring increases with national demand shocks:

$$\frac{dq_{IIfl}}{dp_N} = \underbrace{\frac{\partial q_{IIfl}}{\partial \eta}}_{(-)} \underbrace{\frac{d\eta}{dp_N}}_{(-)} > 0.$$

The intuition for this is that when  $p_N$  rises, the value of entering the lottery rises, too. As more firms enter the lottery instead of selling locally, more firms lose and are forced to flare instead of selling locally.

The effect of pipeline capacity on flaring in a constrained world,  $dq_{IIfl}/dK$  is ambiguous:

$$\frac{dq_{IIfl}}{dK} = \frac{\partial q_{IIfl}}{\partial K} + \frac{\partial q_{IIfl}}{\partial \eta} \frac{d\eta}{dK} = \eta^{-1} \left[ (1 - \eta)(1 - \gamma) - (K - \alpha)\eta^{-1} \underbrace{\frac{d\eta}{dK}}_{(+)} \right]$$

The derivative shows that there are two competing forces. The direct effect— $\partial q_{IIfl}/\partial K$ —is positive since an increase in interruptible capacity on the pipeline  $K - \alpha$  mechanically means more producers attempt to ship via interruptible capacity but are unable to do so and must flare. However, as capacity increases, the probability of being able to get on the pipeline  $\eta$  increases ( $d\eta/dK > 0$ ), and this indirectly lowers the amount flared. When there is little interruptible capacity ( $K - \alpha$  is smaller), the direct effect dominates, and  $dq_{IIfl}/dK > 0$ , but when a larger share of capacity is interruptible ( $K - \alpha$  is bigger), the indirect effect via  $d\eta/dK$  dominates. Having a high probability of being able to sell locally  $\gamma$  also decreases the direct effect and increases the likelihood that additional capacity will reduce flaring.

Since  $c_f$  enters the payoff with a positive sign, a tax on flaring decreases  $c_f$ . Because  $dp_M/dc_f > 0$ , a tax on flaring would lower  $p_M$  as the interruptible lottery became less attractive. Because  $d\eta/dc_f < 0$ , a tax on flaring would increase the probability of “winning” the interruptible lottery and being able to get gas to the national market.

Comparative statics are also important for the price differential  $\lambda = p_N - p_M$ . We can show that the price differential decreases with pipeline capacity  $K$ , and that the price differential does not absorb the entirety of a national demand shock, e.g.,  $d\lambda/dp_N < 1$ .

$$\frac{d\lambda}{dK} = \underbrace{\frac{dp_N}{dK}}_0 - \underbrace{\frac{dp_M}{dK}}_{(+)} < 0 \qquad \frac{d\lambda}{dp_N} = \underbrace{\frac{dp_N}{dp_N}}_1 - \underbrace{\frac{dp_M}{dp_N}}_{(+)} < 1.$$

## D Online Appendix: IV Construction and Robustness

### D.1 Construction of demand shock IV

The intuition behind our demand shock instrument  $Z_{2t}$  is that weather shocks in the rest of the US should increase demand for gas from the Permian most when (a) they are unexpected, and (b) storage in the rest of the US is depleted. We therefore seek to isolate variation in weather that creates unexpected gas demand from the Permian during conditions of depleted storage in the rest of the country. The idea for using weather-driven shocks to storage depletion as an IV for commodity supply and demand models has been articulated and applied in, for example, Roberts and Schlenker (2013) and Hausman and Kellogg (2015), among others. We construct  $Z_{2t}$  from cumulative unexpected national weather shocks over the past year using state-level degree days from NOAA. Both high temperatures (or cooling degree days, CDDs) and low temperatures (or heating degree days, HDDs) increase demand for gas by raising electricity demand and demand for thermal heating. When these weather shocks are expected or transitory, local demand centers may not need to buy additional gas from producing regions like the Permian basin. When the sum of unexpected weather shocks

over the past year is high, storage inventories are likely to be low, and subsequent weather shocks will necessitate pulling gas from producing regions rather than from local storage facilities. In addition, these cumulative weather shocks may only affect gas demand from the Permian if they are “large enough” to have depleted storage. This may occur, for example, if the previous year has had many unexpected shocks to *both* heating and cooling demand, and/or if the cumulative shocks reach a certain threshold so that local gas supply or storage inventories near demand centers is scarce.

With these ideas in mind, in order to construct  $Z_{2t}$  we first separately sum CDDs and HDDs from continental US states that do not border Texas.<sup>31</sup> Denote these “rest of the U.S.” sums as  $cdd_t$  and  $hdd_t$ . Then, we separately regress  $cdd_t$  and  $hdd_t$  on monthly dummies, a time trend, plus the lagged dependent variable (an AR(1) term):

$$cdd_t = \phi + \rho \cdot cdd_{t-1} + \beta \cdot t + \alpha_m + \epsilon_{cdd,t}$$

with a similar regression for  $hdd_t$ . The residuals from each regression  $\epsilon_{cdd,t}$  and  $\epsilon_{hdd,t}$  are unexpected, weather-driven natural gas demand shocks. These demand shocks alone may not affect the demand for transportation out of the Permian basin if storage inventories in the rest of the U.S. are high. Therefore, we next take a running sum of our unexpected weather shocks  $\epsilon_{cdd,t}$  and  $\epsilon_{hdd,t}$  over the previous 365 days, which we will denote  $\delta_{cdd,t} = \sum_{s=1}^{365} \epsilon_{cdd,t-s}$  and  $\delta_{hdd,t} = \sum_{s=1}^{365} \epsilon_{hdd,t-s}$ . These cumulative sums of unexpected weather shocks over the last year can be thought of as exogenous shocks to gas storage inventories. For a storable commodity, unexpected inventory changes are the relevant shock for a constrained delivery system. Further, cold weather streaks (cumulative HDD shocks) must be large enough to deplete storage, and will matter more for a constrained system when there have also been hot weather streaks (cumulative CDD shocks) in the same period, particularly when the heating demand shocks are large, because both types of shocks deplete storage and affect demand for gas from producing basins. Consistent with this, we observe empirically that below a certain level the cumulative HDD shock is unrelated to the price differential (as shown in Appendix Figure D.1), likely because in this range there is surplus gas available in storage around the country to handle short-term demand shocks without increasing demand from the Permian. In constructing our instrument, we shift our heating demand shocks  $\delta_{hdd,t}$  to adjust for this. To capture all of these ideas, we construct our weather instrument as

$$Z_{2t} = \max\{0, \delta_{cdd,t} + \delta_{hdd,t}\} + \max\{0, \delta_{cdd,t}\} \cdot \max\{0, \delta_{hdd,t} + 25\}.$$

## D.2 Relevance and validity of demand shock IV

Appendix Figure D.2 demonstrates instrument relevance for  $Z_{2t}$  through the clearly strong relationship between this cumulative weather-driven storage inventory shock IV versus the endogenous Henry Hub/Waha price differential. The IV explains more than half of the variation in the price differential.

The relevance of  $Z_{2t}$  for congestion is also illustrated in Figure D.3. Panel (a) shows that the positive relationship between interstate pipeline capacity utilization and  $Z_{2,t}$  explains

---

<sup>31</sup>We exclude CO, KS, LA, NM, OK, and TX.

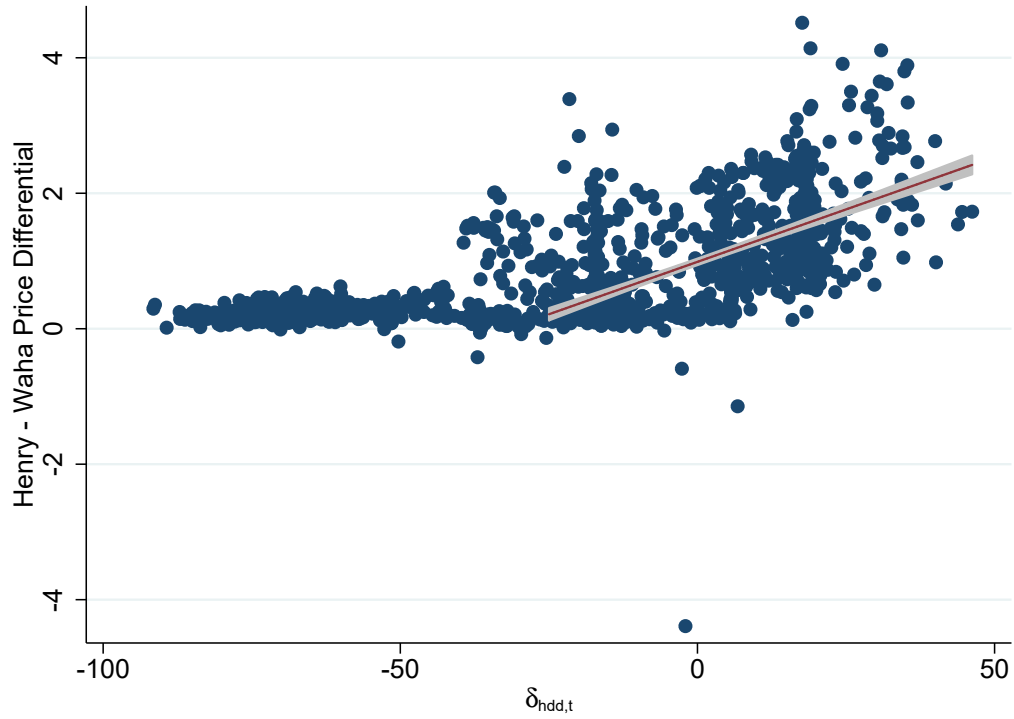
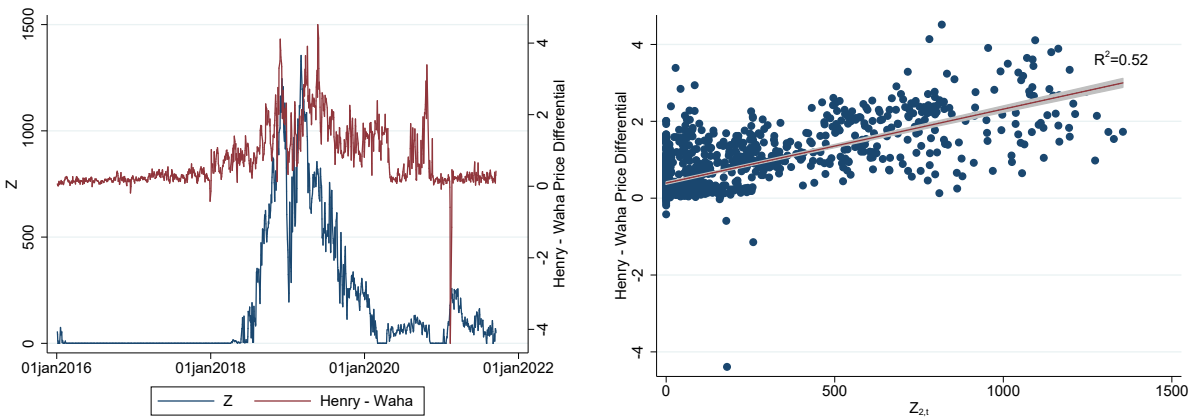


Figure D.1: Running 365-day sum of unexpected heating degree day shocks ( $\delta_{hdd,t}$ ) vs. Henry Hub - Waha price differential



(a) Time series

(b) Scatter and Linear Fit

Figure D.2: Instrument  $Z_{2t}$  vs. Henry Hub–Waha price differential  $\Delta p_t$

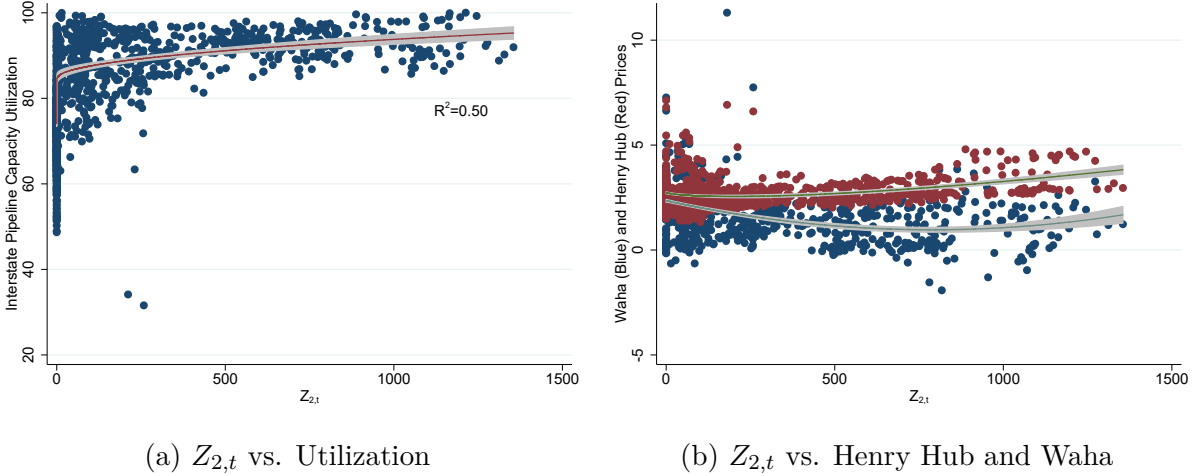


Figure D.3: Instrument  $Z_{2,t}$  vs. Interstate Pipeline Capacity Utilization and Hub Prices. Fitted lines are second-order fractional polynomials.

about half of the variation in utilization. Although this ignores intrastate capacity, it corroborates the argument that  $Z_{2,t}$  affects congestion. Panel (b) of Figure D.3 shows that the Henry Hub price (in red) is moderately increasing throughout the range of  $Z_{2,t}$ , as would be expected with rest-of-US demand shocks. The Waha price (in blue) on the other hand is declining over low levels of  $Z_{2,t}$ , i.e., when congestion is low, but then is flat or increasing over moderate to high levels of  $Z_{2,t}$  when congestion is higher. This is consistent with some new supply being offered to the market at low levels of congestion, either from new production or from holders of inventories in the Permian, but it is also consistent with our finding that gas-directed wells in the Permian reduce supply when congestion increases. We will also show this in the relationship between  $Z_{2,t}$  and our daily fracking activity controls.

The biggest threat to the exclusion restriction on  $Z_{2,t}$  is that national demand shocks could induce flaring and methane emissions from new production from new wells. Figure D.4 helps alleviate this concern by showing the relationship between  $Z_{2,t}$  and three daily fracking activity measures: total number of fracking jobs in Panel (a), fracking water used in Panel (b), and proppant used in fracking in Panel (c). In all three cases, these activity measures rise over low levels of  $Z_{2,t}$ , i.e., when congestion is low, but they are flat or declining at moderate to higher levels, i.e., when congestion is occurring. This suggests that the exclusion restriction is likely to hold under conditions of interest, i.e., congested conditions. The decline in production activity measures at higher congestion is also consistent with our well-level results in Section 4 showing that gas-directed wells reduce output when congestion occurs.

If the exclusion restriction is violated and  $Z_{2,t}$  affects flaring and methane through new production activity, then conditioning on production activity in the second stage should close this channel. Table D.1 reports results from the same IV specifications as in Table 1, but with the inclusion of these daily activity variables in the second stage. In all cases, coefficients in Table D.1 as well as diagnostic statistics ( $R^2$ , first-stage KP-F statistics, and overidentification tests) are very close in magnitude and almost always the same statistical significance as in Table 1. These results are also robust to estimating Panels A and D using Poisson regression to account for zero values in flaring detections or methane emissions cal-

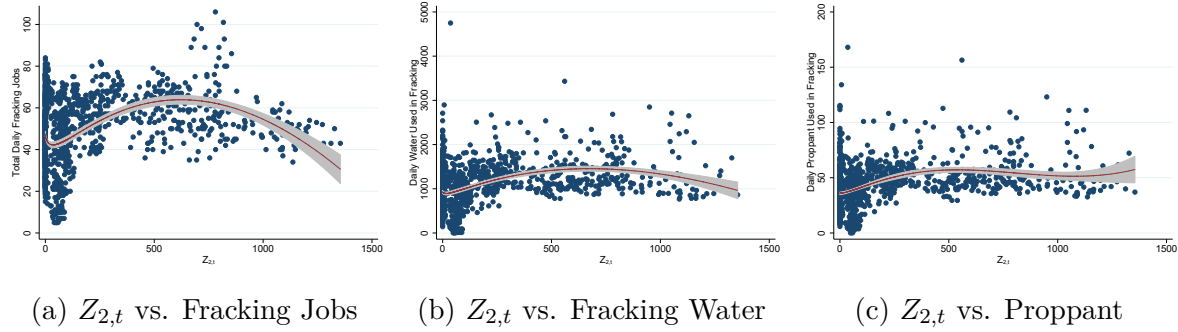


Figure D.4: Instrument  $Z_{2,t}$  vs. Daily Fracking Activity Measures. Fitted lines are third-order fractional polynomials.

culations, and to including quadratic terms and lags in the fracking activity control variables. Those additional robustness checks are available upon request.

Finally, Table D.2 reports results with heterogeneous effects by congestion status. We define a congestion dummy variable that is equal to 1 when the interstate pipeline capacity utilization is greater than 90 percent, and zero otherwise. We then include two treatment variables,  $\Delta p_t \cdot D$  for the slope during congestion and  $\Delta p_t \cdot (1 - D)$  for the slope without congestion. We similarly redefine each IV with these interactions. In the second stage we also control for the three fracking activity measures and their interactions with the congestion dummy. In the methane regressions (Panels B, C, and D) we find in all cases that the coefficients under congestion are much larger in magnitude and more often significant than the coefficients without congestion. In the flaring regressions (Panel A) we find somewhat smaller effects during congestion but they are still strongly statistically significant and similar in magnitude to our preferred estimates in Table 1. Tables D.1 and D.2, as well as Figures D.3 and D.4, together help us conclude that our main results in Table 1 are not contaminated by exclusion restriction violations from flaring and methane due to new production activity.

Table D.1: Impact of Henry Hub-Waha Price Differential on Flaring and Methane: Time Series with Fracking Controls

	OLS	$Z_{1t}$	$Z_{2t}$	$Z_{1t}, Z_{2t}$
<b>Panel A: Log Flaring</b>				
$\Delta p_t$	0.58*** (0.063)	0.95*** (0.29)	0.73*** (0.10)	0.74*** (0.10)
$R^2$	0.25	0.23	0.25	0.25
KP - F Stat		9.81	57.0	40.7
Hansen's J p-value				0.42
N = 1278				
<b>Panel B: Log Methane Concentrations</b>				
$\Delta p_t$	0.00029 (0.00040)	0.0086 (0.0098)	0.0017 (0.0012)	0.0019 (0.0012)
$R^2$	0.48	0.23	0.47	0.47
KP - F Stat		1.53	28.0	15.3
Hansen's J p-value				0.33
N = 715				
<b>Panel C: Methane Emissions</b>				
$\Delta p_t$	2.18 (4.23)	98.1 (110.7)	16.1 (12.3)	18.2 (12.1)
$R^2$	0.51	0.23	0.50	0.50
KP - F Stat		1.53	32.7	17.4
Hansen's J p-value				0.30
N = 715				
<b>Panel D: Log Methane Emissions</b>				
$\Delta p_t$	0.070*** (0.025)	0.52 (0.57)	0.24*** (0.083)	0.25*** (0.081)
$R^2$	0.42	0.21	0.39	0.39
KP - F Stat		1.75	35.6	19.0
Hansen's J p-value				0.52
N = 699				

**Notes:**  $\Delta p_t$  is the Henry Hub - Waha price differential. All regressions include a linear trend and monthly dummies, and three daily fracking activity control variables: the number of active fracking jobs, and the quantities of water and proppant used in fracking. Panel A reports results for the log of flaring, Panel B for the log of methane concentrations, Panel C for methane emissions, and Panel D for the log of methane emissions. Column 1 reports OLS estimates. Column 2 uses  $Z_{1t}$ , the presence of a pipeline maintenance event, as an IV for  $\Delta p_t$ . Column 3 uses  $Z_{2t}$ , the cumulative unexpected weather shocks proxying storage depletion, as an IV. Column 4 uses both IVs. HAC standard errors in parentheses. \*\*\* indicates significance at the 1% level, \*\* at the 5% level, \* at the 10% level.

Table D.2: Impact of Henry Hub-Waha Price Differential on Flaring and Methane by Congestion Status

	$Z_{2t}$	$Z_{1t}, Z_{2t}$	$Z_{2t}$	$Z_{1t}, Z_{2t}$
	<b>Panel A: Log Flaring</b>		<b>Panel B: Log Methane Conc.</b>	
$\Delta p_t$ - Uncongested	0.88*** (0.14)	0.95*** (0.15)	-0.00040 (0.0014)	-0.00039 (0.0015)
$\Delta p_t$ -Congested	0.67*** (0.17)	0.63*** (0.16)	0.0030 (0.0018)	0.0032* (0.0018)
$R^2$	0.25	0.25	0.47	0.46
KP - F Stat	14.3	9.62	10.3	6.76
Hansen's J p-value		0.15		0.66
N		1278		715
	<b>Panel C: Methane Emiss.</b>		<b>Panel D: Log Methane Emiss.</b>	
$\Delta p_t$ - Uncongested	-8.61 (14.8)	-8.42 (15.4)	0.16** (0.079)	0.13 (0.080)
$\Delta p_t$ -Congested	30.4 (19.3)	33.0* (18.9)	0.29** (0.12)	0.31*** (0.11)
$R^2$	0.49	0.49	0.39	0.39
KP - F Stat	10.9	6.84	15.8	9.22
Hansen's J p-value		0.63		0.32
N		715		699

**Notes:**  $\Delta p_t$  is the Henry Hub - Waha price differential. The “Congested” periods are defined by a dummy equal to one if the interstate pipeline utilization is greater than 90 percent. Coefficients are reported as the slope in a given regime, i.e., coefficients do not need to be added together. All regressions include a linear trend and monthly dummies, and interactions of three daily fracking activity control variables with the congestion dummy: the number of active fracking jobs, and the quantities of water and proppant used in fracking. Panel A reports results for the log of flaring, Panel B for the log of methane concentrations, Panel C for methane emissions, and Panel D for the log of methane emissions. Column 1 reports OLS estimates. Column 2 uses  $Z_{1t}$ , the presence of a pipeline maintenance event, as an IV for  $\Delta p_t$ . Column 3 uses  $Z_{2t}$ , the cumulative unexpected weather shocks proxying storage depletion, as an IV. Column 4 uses both IVs. HAC standard errors in parentheses. \*\*\* indicates significance at the 1% level, \*\* at the 5% level, \* at the 10% level.

## E Online Appendix: Additional Figures and Tables

Table E.1: Production, flaring, and reported value of production from Permian Wells.

Year	Total production		Disposition	Reported revenue			
	Oil (mmbbl/d)	Gas (bcf/d)	Flaring (bcf/d)	Oil (\$million/d)	Gas (\$million/d)	Ratio	Gas price (\$/mcf)
2007	0.68	3.2	0.01	47	21	2.3	6.47
2008	0.70	3.3	0.01	68	26	2.7	7.73
2009	0.70	3.3	0.01	41	12	3.4	3.67
2010	0.73	3.1	0.01	56	15	3.8	4.72
2011	0.81	3.0	0.03	74	16	4.6	5.35
2012	0.94	3.2	0.05	83	13	6.6	3.99
2013	1.07	3.5	0.09	99	15	6.4	4.47
2014	1.29	4.2	0.12	108	20	5.3	4.83
2015	1.47	4.9	0.19	66	12	5.6	2.40
2016	1.61	5.3	0.17	64	14	4.7	2.60
2017	2.00	6.4	0.18	97	23	4.2	3.58
2018	2.80	8.6	0.35	160	31	5.1	3.61
2019	3.44	11.3	0.47	186	24	7.6	2.17
2020	3.44	12.4	0.26	127	23	5.5	1.91
2021	3.48	13.1	0.17	234	66	3.6	4.96
2022	3.75	14.5	0.19	358	100	3.6	6.90

Data sources are TX RRC for production and flaring, and Enverus for value, which is derived from TX Comptroller data. Since not all wells were matched to comptroller data, we scale up value by the ratio of production reported to RRC to production reported to comptroller. Dollar values are in nominal terms.

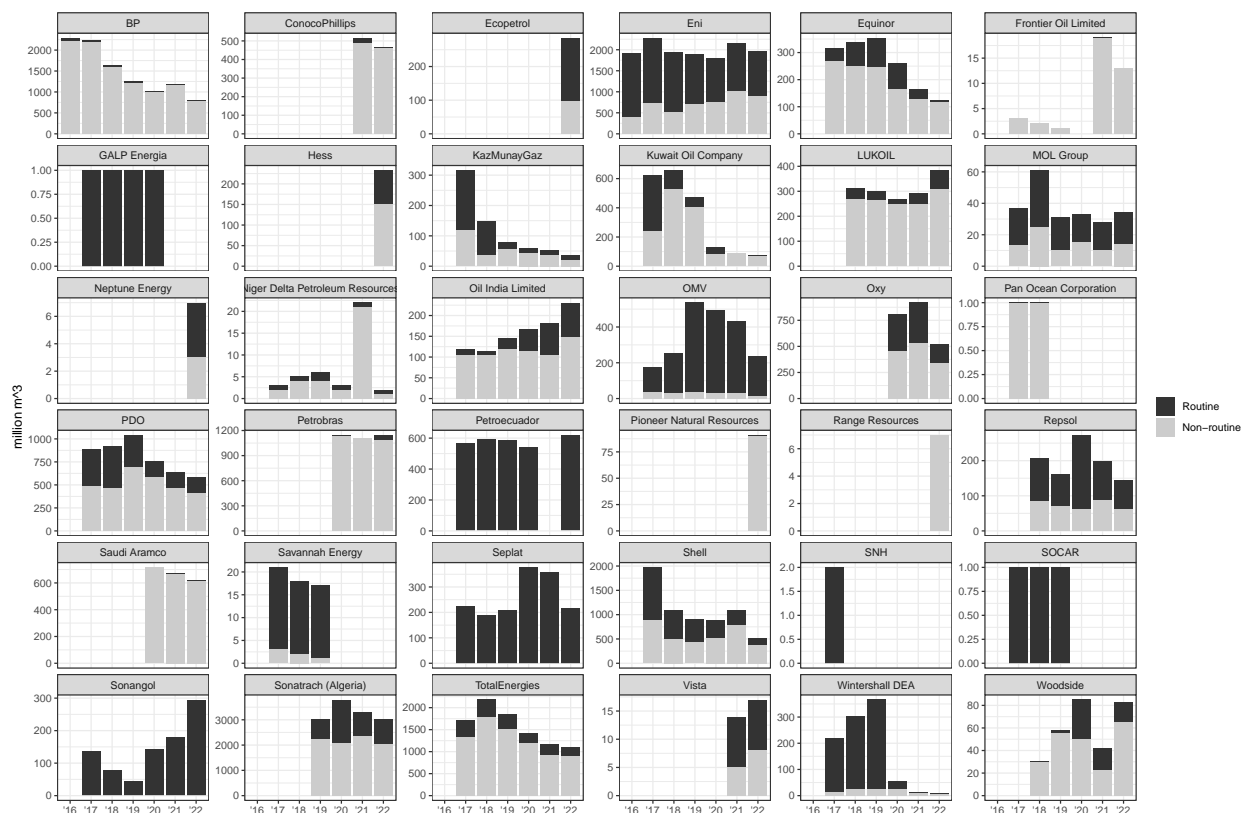


Figure E.1: Self-reported flaring volumes by companies endorsing the World Bank Zero Routine Flaring by 2030 initiative. Data downloaded from <https://www.worldbank.org/en/programs/zero-routine-flaring-by-2030/reporting>

Share of gas sold	Flaring (bcf)	Share
(0.75, 1]	224.5	0.40
(0.5, 0.75]	109.0	0.19
(0.25, 0.5]	66.9	0.12
[0, 0.25] (Connected)	104.4	0.19
[0, 0.25] (Unconnected)	57.3	0.10

Production data are from Nov 2015 through May 2021. Well-month observations are classified based on the share of gas reported as sold in the disposition report relative to monthly production. Note that production is reported at the gas-well and oil-lease level (see discussion in Section 2.3).

Table E.2: Permian flaring by share of gas production sold in the same month (Nov 2015–May 2021)

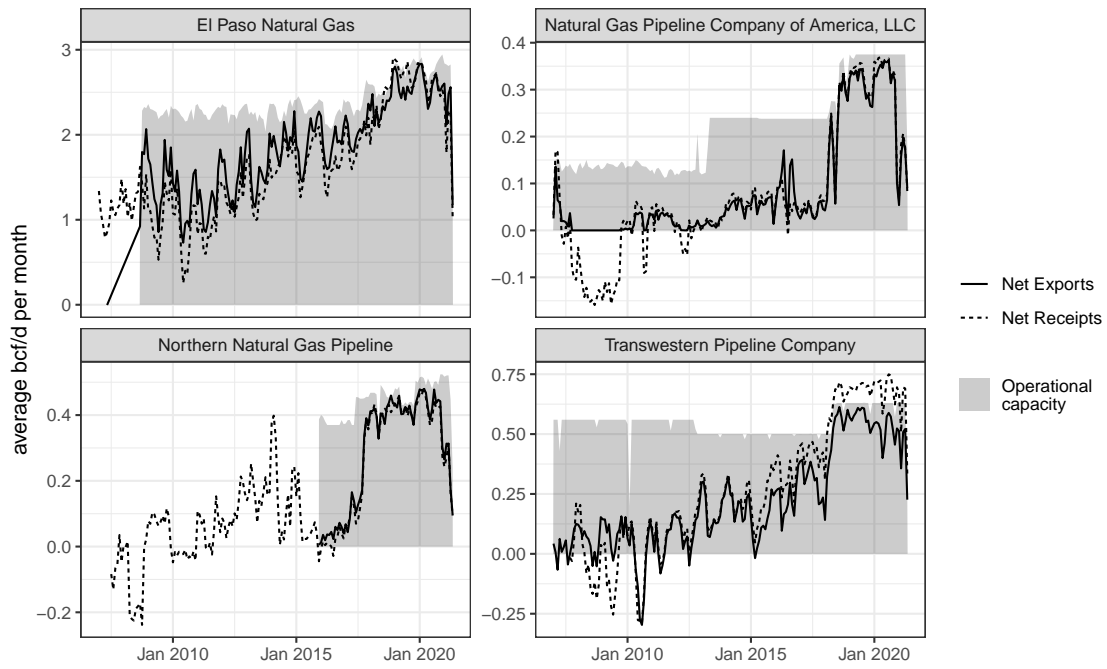


Figure E.2: Net receipts, net exports, and operational capacity for Permian interstate systems

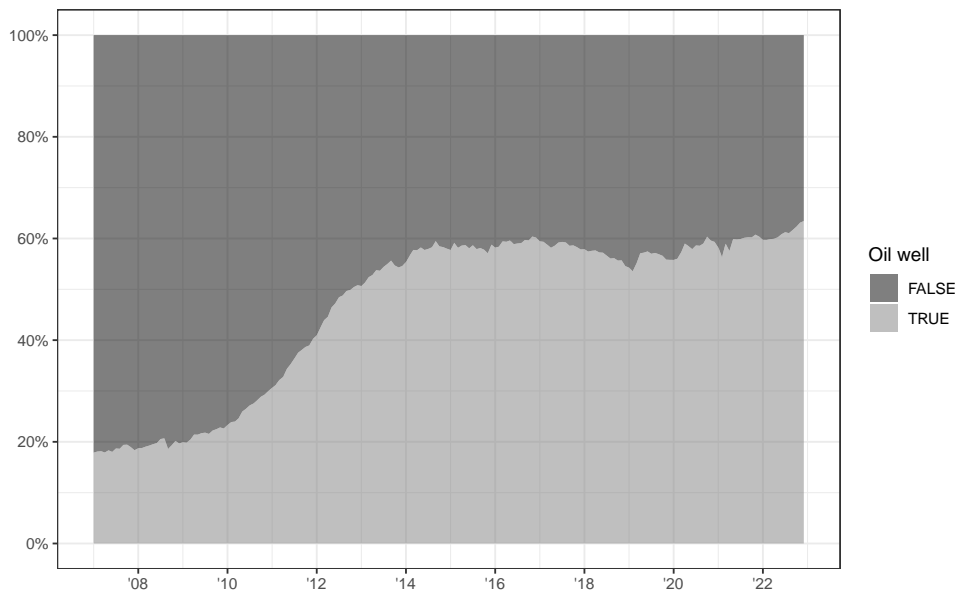


Figure E.3: Share of Texas Permian gas production from oil-designated wells

Table E.3: Climate costs of flaring associated gas following latest GHGRP Subpart W under current and previous SC-GHGs from U.S. EPA (2023) and IAWG (2021)

Current U.S. EPA (2023): Total (CH <sub>4</sub> + CO <sub>2</sub> )		
Destruction efficiency	Associated gas	Pure CH <sub>4</sub>
Perfect combustion	\$15.95 (0.00 + 15.95)	\$10.18 (0.00 + 10.18)
98% (Tier 1)	\$15.81 (0.42 + 15.40)	\$10.45 (0.63 + 9.82)
95% (Tier 2)	\$15.96 (1.05 + 14.92)	\$11.09 (1.58 + 9.52)
92% (Tier 3)	\$16.11 (1.67 + 14.44)	\$11.74 (2.53 + 9.21)
0% (Venting)	\$20.95 (20.91 + 0.03)	\$31.56 (31.56 + 0.00)
Previous IAWG (2021): Total (CH <sub>4</sub> + CO <sub>2</sub> )		
Destruction efficiency	Associated gas	Pure CH <sub>4</sub>
Perfect combustion	\$4.22 (0.00 + 4.22)	\$2.69 (0.00 + 2.69)
98% (Tier 1)	\$4.45 (0.38 + 4.08)	\$3.17 (0.57 + 2.60)
95% (Tier 2)	\$4.89 (0.94 + 3.95)	\$3.94 (1.42 + 2.52)
92% (Tier 3)	\$5.33 (1.51 + 3.82)	\$4.71 (2.28 + 2.44)
0% (Venting)	\$18.86 (18.85 + 0.01)	\$28.44 (28.44 + 0.00)

Each cell shows the total climate cost, as well as the separate methane and CO<sub>2</sub> components. Since associated gas can contain CO<sub>2</sub>, even fully vented associated gas has a non-zero CO<sub>2</sub> climate cost. We take our Permian associated gas composition from Howard et al. (2015) Table 2. We assume standard oilfield temperature and pressures of 60°F and 14.65 psia (288.706K and 1.01008 kPa) according to reporting requirements in Texas (Tex. Admin. Code 16, § 3.79) and use the CoolProp library (Bell et al. 2014) to calculate gas densities. The table shows social costs using the latest SCC and SCM for 2020 emissions in 2020 USD under the recommended 2% discount rate from U.S. EPA (2023) (\$193/t and \$1648/t), as well as the previous SCC and SCM from IAWG (2021) under a 3% discount rate (\$51/t and \$1485/t). We calculate CO<sub>2</sub> and CH<sub>4</sub> emissions per updated GHRP Subpart W (U.S. EPA 2024). One notable change in U.S. EPA (2024) is the assumption that combustion efficiency (conversion of hydrocarbons into CO<sub>2</sub>) equals destruction efficiency (destruction of CH<sub>4</sub>) minus 1.5%. A significant change relative to Agerton et al. (2023) is that we follow the GHGRP and assume that the GWP of ethane, propane, and butane are zero. Agerton et al. (2023) takes GWP for these hydrocarbons from Hodnebrog et al. (2018). We note that Table 7.SM.6 from IPCC 2021 (AR 6) Ch 7 Supplementary Materials specifies negligible GWPs for these hydrocarbons (Masson-Delmotte et al. 2021). Values in parentheses show the breakdown of social costs from (vented CH<sub>4</sub> + CO<sub>2</sub> from combustion). The “perfect combustion” scenario is infeasible and assumes that both combustion and destruction efficiency are 100%.

Table E.4: Relationship Between Satellite Detections of Flaring and Methane

Dependent Variable:	Methane Concentration	Log Methane Concentration	Methane Emissions	Methane Emissions
Flaring	0.030*** (0.0065)		0.18*** (0.039)	
Log(Flaring)		0.00054*** (0.000083)		5.92*** (0.91)
r <sup>2</sup>	0.45	0.45	0.48	0.48
N = 15883				

**Notes:** Std. errors clustered at the grid cell level. All regressions include cell-by-month and cell-by-year fixed effects. Results are robust to many alternative fixed effect specifications, subsamples, and definitions of the left and right hand side variables. \*\*\* indicates significance at the 1% level, \*\* at the 5% level, \* at the 10% level.

Table E.5: Impact of Unplanned Pipeline Maintenance Events on Flaring and Methane

	Poisson Flaring	Log Methane Concentrations	Methane Emissions	Pois Methane Emissions
-3	0.18 (0.26)	0.0013 (0.0018)	15.1 (20.3)	0.019 (0.067)
-2	-0.17 (0.27)	0.00060 (0.0022)	7.24 (24.5)	-0.0013 (0.077)
-1	-	-	-	-
0	0.65* (0.37)	0.0054* (0.0030)	61.7* (34.5)	0.22*** (0.074)
1	-0.28 (0.24)	-0.000012 (0.0018)	-0.39 (20.4)	-0.041 (0.068)
2	0.027 (0.21)	-0.0010 (0.0015)	-12.2 (17.5)	-0.056 (0.059)
3	0.34 (0.22)	0.00039 (0.0016)	2.64 (17.3)	-0.042 (0.056)
N	130	135	135	135
r <sup>2</sup>		0.50	0.52	

**Notes:** Time series event study coefficients shown in Figure 8. Flaring regressions include a time trend; methane regressions include monthly dummies and a time trend. Columns 2 and 3 are estimated by OLS, and report HAC standard errors with automatic bandwidth. Columns 1 and 4 are estimated using Poisson regression to handle days with zeros in the satellite flaring data or in our methane emissions calculations, and report heteroskedasticity-robust standard errors. Results are generally robust to dropping the trend, using OLS on levels or logs of all dependent variables (with dropped observations for zeros in logged outcomes), and controlling for daily fracking activity, water, and proppant use. \* 0.10 \*\* 0.05 \*\*\* 0.01.

Table E.6: Impact of Unplanned Pipeline Maintenance Events on Flaring: Robustness Checks

	Level	Log (OLS)	Log (OLS)	Poisson	Level	Log (OLS)	Log (OLS)	Poisson
-3	40.4 (43.8)	0.58 (0.67)	0.82 (0.64)	0.32 (0.25)	64.0 (43.6)	0.70 (0.70)	0.93 (0.66)	0.45* (0.25)
-2	-45.6 (47.4)	-0.39 (0.55)	-0.40 (0.55)	-0.28 (0.26)	-32.9 (48.8)	-0.29 (0.55)	-0.30 (0.56)	-0.22 (0.28)
-1	-	-	-	-	-	-	-	-
0	119.2 (79.4)	1.49** (0.70)	1.68** (0.71)	0.64* (0.36)	118.1 (74.1)	1.49** (0.69)	1.58** (0.70)	0.67** (0.33)
1	-39.5 (41.1)	-0.12 (0.54)	-0.047 (0.56)	-0.24 (0.24)	-36.4 (40.4)	-0.066 (0.54)	-0.075 (0.56)	-0.20 (0.21)
2	11.1 (38.4)	-0.046 (0.41)	-0.013 (0.44)	0.068 (0.20)	30.2 (38.9)	0.023 (0.40)	0.058 (0.42)	0.15 (0.18)
3	41.3 (37.0)	0.86 (0.59)	1.01* (0.61)	0.32 (0.22)	63.7 (39.3)	1.01 (0.61)	1.12* (0.63)	0.44* (0.23)
Trend	YES	YES	NO	YES	YES	YES	NO	YES
Controls	NO	NO	NO	NO	YES	YES	YES	YES
N	124	124	124	124	124	124	124	124
r <sup>2</sup>	0.17	0.14	0.084	0.26	0.16	0.13		

**Notes:** Robustness checks for time series event studies. Columns 1 to 3 and 5 to 7 are estimated by OLS, and report HAC standard errors with automatic bandwidth. Columns 4 and 8 are estimated using Poisson regression to handle days with zeros in the satellite flaring data, and report heteroskedasticity-robust standard errors. Control variables include the daily number of active fracking jobs, and the daily amount of water and proppant used in fracking. \* 0.10 \*\* 0.05 \*\*\* 0.01.

Table E.7: Impact of Unplanned Pipeline Maintenance Events on Methane: Robustness Checks

	Methane Concentrations	Log Methane Concentrations	Methane Emissions	Log Methane Emissions	Pois Methane Emissions
Panel A: No Fracking Controls					
-3	2.54 (3.35)	0.0013 (0.0018)	15.1 (20.3)	-0.021 (0.13)	0.042 (0.063)
-2	1.12 (4.08)	0.00060 (0.0022)	7.24 (24.5)	0.11 (0.20)	0.022 (0.083)
-1	-	-	-	-	-
0	10.2* (5.65)	0.0054* (0.0030)	61.7* (34.5)	0.18 (0.13)	0.19** (0.086)
1	-0.0077 (3.32)	-0.000012 (0.0018)	-0.39 (20.4)	0.012 (0.11)	-0.0052 (0.070)
2	-1.89 (2.83)	-0.0010 (0.0015)	-12.2 (17.5)	-0.065 (0.099)	-0.041 (0.059)
3	0.74 (2.91)	0.00039 (0.0016)	2.64 (17.3)	-0.045 (0.096)	-0.0033 (0.057)
N	135	135	135	133	135
r2	0.51	0.50	0.52	0.33	
Panel B: With Fracking Controls					
-3	0.97 (3.49)	0.00049 (0.0019)	6.32 (21.3)	-0.060 (0.14)	0.019 (0.067)
-2	-0.019 (3.88)	-0.0000096 (0.0021)	0.29 (23.3)	0.063 (0.18)	-0.0013 (0.077)
-1	-	-	-	-	-
0	10.9** (4.77)	0.0058** (0.0025)	66.3** (29.4)	0.21* (0.11)	0.22*** (0.074)
1	-1.76 (3.29)	-0.00096 (0.0018)	-10.9 (20.1)	-0.050 (0.11)	-0.041 (0.068)
2	-2.63 (2.86)	-0.0014 (0.0015)	-16.5 (17.6)	-0.081 (0.096)	-0.056 (0.059)
3	-1.23 (2.93)	-0.00067 (0.0016)	-9.04 (17.6)	-0.11 (0.088)	-0.042 (0.056)
N	135	135	135	133	135
r2	0.54	0.54	0.56	0.38	

**Notes:** Robustness checks for time series event studies. Columns 1 to 4 are estimated by OLS, and report HAC standard errors with automatic bandwidth. Column 5 is estimated using Poisson regression to handle days with zeros in our methane emissions calculations, and reports heteroskedasticity-robust standard errors. Panel B includes control variables on the daily number of active fracking jobs, and the daily amount of water and proppant used in fracking. \* 0.10 \*\* 0.05 \*\*\* 0.01.

Table E.8: Well Summary Statistics

	<i>N</i>	Mean	Std. Dev.	Min	Max
<b>Panel A: Oil Leases</b>					
Flaring (mcf)	409498	290.25	2654.25	0	248003
Gas Pdxn (mcf)	409498	8670.24	25905.53	0	1234003
Oil Pdxn (bbl)	409498	3267.71	10740.88	0	460993
Maintenance Event	409498	0.023	0.05	0	0.33
Vertically Integrated	409498	0.005	0.073	0	1
Gas Price Sold	143612	3.56	1.28	0.179	6.540
<b>Panel B: Gas Wells</b>					
Flaring (mcf)	180629	457.041	3271.10	0	261479
Gas Pdxn (mcf)	180629	14950.39	34094.34	0	683244
Oil Pdxn (bbl)	180629	1830.57	4913.34	0	121066
Maintenance Event	180629	0.01	0.03	0	0.33
Vertically Integrated	180629	0.003	0.06	0	1
Gas Price Sold	68327	3.15	1.26	0.184	6.532

**Notes:** This table reports summary statistics from the TRCC well and lease data. Vertically integrated is an indicator that takes a value of one if the well operator and connected gas plant share the same parent firm. Gas Price Sold is calculated by dividing the total value of gas sold by the volume sold from a well in a given month. Maintenance event is a binary variable that takes a value of one if the plant the well is closest to via gathering line distance is connected to a transmission line that experienced an unanticipated maintenance event that month.

**Sample:** Self-reported month level observations of leases and wells from December 2015 ending in 2021. Panel A presents statistics from leases or wells that are primarily oil-producing. Panel B presents statistics from leases or wells that are primarily gas-producing.

Table E.9: Primary Results: Impact of Pipeline Events on Well Activity

	Log(Throughput)			Log(Capacity)		
	All (1) b/se	NGPL Only (2) b/se	No NGPL (3) b/se	All (4) b/se	NGPL Only (5) b/se	No NGPL (6) b/se
-3	0.017 (0.051)	0.125 (0.135)	-0.042 (0.029)	0.022 (0.043)	0.185 (0.174)	0.002 (0.010)
-3	-0.001 (0.044)	0.041 (0.122)	-0.000 (0.021)	0.030 (0.046)	0.189 (0.175)	0.003 (0.004)
-1	-	-	-	-	-	-
0	-0.147* (0.086)	-0.150 (0.098)	-0.085 (0.062)	-0.146 (0.123)	-0.163 (0.159)	-0.058** (0.025)
1	-0.047** (0.023)	-0.021 (0.024)	-0.030 (0.019)	-0.043* (0.025)	-0.033 (0.026)	-0.016* (0.008)
2	0.032 (0.033)	0.086 (0.076)	-0.002 (0.016)	-0.013 (0.012)	0.043 (0.052)	-0.003 (0.005)
3	0.019 (0.035)	0.064 (0.066)	0.008 (0.035)	-0.024 (0.015)	0.051 (0.052)	-0.011 (0.010)
<i>N</i>	1114	538	576	1114	538	576
adj. <i>R</i> <sup>2</sup>	0.713	0.639	0.902	0.285	0.145	0.931
Pipeline FE	Y	-	Y	Y	-	Y
Month FE	Y	Y	Y	Y	Y	Y
Pipeline-Time Trends	Y	Y	Y	Y	Y	Y

**Notes:** This table reports estimates the impact of a maintenance event for the interstate transmission line using our baseline equation. Columns (1) - (3) consider the outcome of log of exports (throughput), columns (3) to (6) consider the log of reported operational capacity. Columns (2), (3), (5), and (6) break up the sample by Natural Gas Pipeline of America observations or not. We use one-way pipeline-month-level clustered standard errors. \*\*\* indicates significance at the 1% level, \*\* at the 5% level, and \* at the 10% level.

**Sample:** pipeline-day level data from the Woodmac beginning in December 2015 and ending in 2021. We only include the 1,114 observations within a clean event window during the sample timeframe. A clean event window is when no other event is ongoing within a three day window before and exclude any post event days where a new event begins.

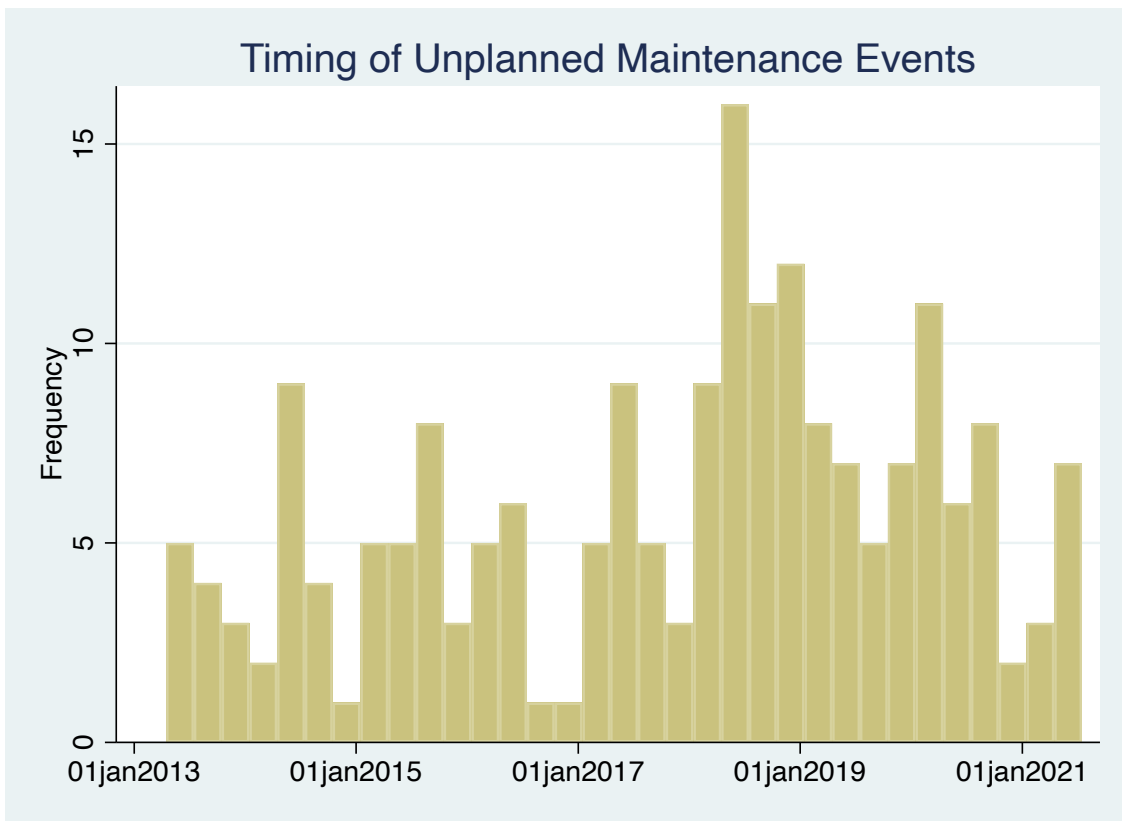
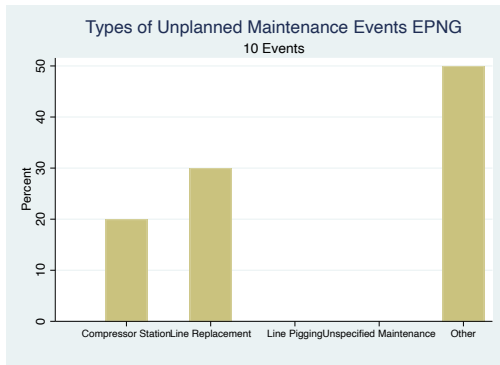
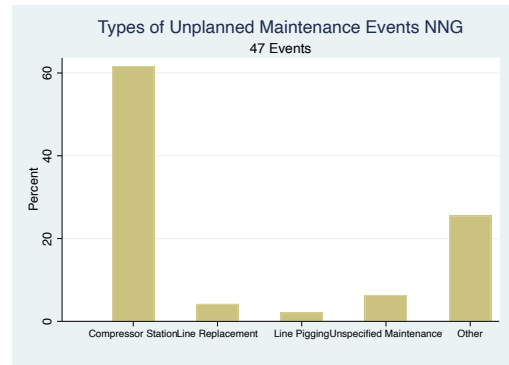


Figure E.4: Maintenance Events over Time

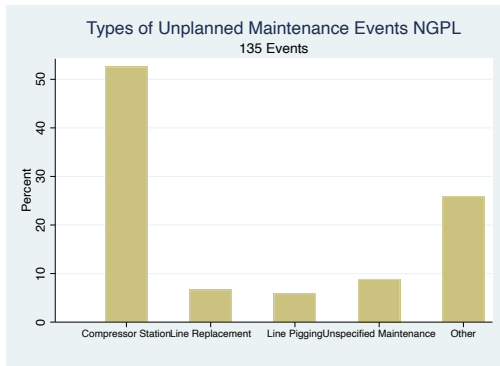
Figure E.5: Maintenance Events by Pipeline



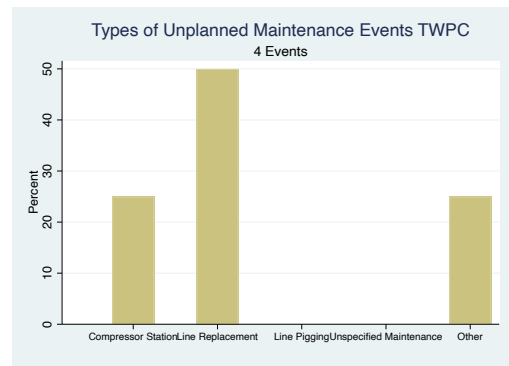
(a) El Paso Natural Gas



(b) Northern Natural Gas



(c) Natural Gas Pipeline Company of America



(d) Transwestern Pipeline

## Online Appendix: References

- Agerton, Mark, Ben Gilbert, and Gregory B. Upton (2023). “The Economics of Natural Gas Flaring and Methane Emissions in US Shale: An Agenda for Research and Policy”. *Review of Environmental Economics and Policy* 17.2, 251–273. DOI: [10.1086/725004](https://doi.org/10.1086/725004).
- American Gas Association (2007). *Ratemaking for Energy Pipelines*. American Gas Association.
- Barkley, Zachary, Kenneth Davis, Natasha Miles, et al. (2022). “Quantification of Oil and Gas Methane Emissions in the Delaware and Marcellus Basins Using a Network of Continuous Tower-Based Measurements”. *Atmospheric Chemistry and Physics Discussions*, 1–25. DOI: [10.5194/acp-2022-709](https://doi.org/10.5194/acp-2022-709).
- Bell, Ian H., Jorrit Wronski, Sylvain Quoilin, and Vincent Lemort (2014). “Pure and Pseudopure Fluid Thermophysical Property Evaluation and the Open-Source Thermophysical Property Library CoolProp”. *Industrial & Engineering Chemistry Research* 53.6, 2498–2508. DOI: [10.1021/ie4033999](https://doi.org/10.1021/ie4033999).
- Cremer, Helmuth and Jean-Jacques Laffont (2002). “Competition in Gas Markets”. *European Economic Review* 46.4, 928–935. DOI: [10.1016/S0014-2921\(01\)00226-4](https://doi.org/10.1016/S0014-2921(01)00226-4).
- Cusworth, Daniel H, Andrew K Thorpe, Alana K Ayasse, et al. (2022). “Strong methane point sources contribute a disproportionate fraction of total emissions across multiple basins in the United States”. *Proceedings of the National Academy of Sciences* 119.38, e2202338119.
- Followill, Becca, David Pursell, and Anson Williams (2008). *Midstream Update & Primer*. Slide deck. Tudor Pickering Holt & Co.
- Hausman, Catherine and Ryan Kellogg (2015). *Welfare and distributional implications of shale gas*. Tech. rep. National Bureau of Economic Research.
- Hodnebrog, Øivind, Stig B. Dalsøren, and Gunnar Myhre (2018). “Lifetimes, Direct and Indirect Radiative Forcing, and Global Warming Potentials of Ethane (C<sub>2</sub>H<sub>6</sub>), Propane (C<sub>3</sub>H<sub>8</sub>), and Butane (C<sub>4</sub>H<sub>10</sub>)”. *Atmospheric Science Letters* 19.2, e804. DOI: [10.1002/asl.804](https://doi.org/10.1002/asl.804).
- Howard, Touché, Thomas W. Ferrara, and Amy Townsend-Small (2015). “Sensor Transition Failure in the High Flow Sampler: Implications for Methane Emission Inventories of Natural Gas Infrastructure”. *Journal of the Air & Waste Management Association* 65.7, 856–862. DOI: [10.1080/10962247.2015.1025925](https://doi.org/10.1080/10962247.2015.1025925).
- IAWG (2021). *Social Cost of Carbon, Methane, and Nitrous Oxide Interim Estimates under Executive Order 13990*. Technical Support Document. Interagency Working Group on Social Cost of Greenhouse Gases, 48.
- Kafka, Greg and Jim Strawn (2017). *Acquiring Midstream Assets And Gas Agreements Part 1 and 2.Pdf*. Law360. URL: <https://m.winstead.com/portalresource/lookup/poid/Z1t019NPluKPtDNIqLMRVPMQiLsSwKZCmG3!/document.name=/Acquiring%20Midstream%20Assets%20And%20Gas%20Agreements%20Part%201%20and%202.pdf>.
- Masson-Delmotte, Valérie, Panmao Zhai, Anna Pirani, et al., eds. (2021). *Climate Change 2021: The Physical Science Basis. Contribution of Working Group I to the Sixth Assessment Report of the Intergovernmental Panel on Climate Change*. Cambridge, United Kingdom and New York, NY, USA: Cambridge University Press. DOI: [10.1017/9781009157896](https://doi.org/10.1017/9781009157896).

- Mohlin, Kristina (2021). “The U.S. Gas Pipeline Transportation Market: An Introductory Guide with Research Questions for the Energy Transition”. *SSRN Electronic Journal*. DOI: [10.2139/ssrn.3775725](https://doi.org/10.2139/ssrn.3775725).
- Oliver, Matthew E., Charles F. Mason, and David Finnoff (2014). “Pipeline Congestion and Basis Differentials”. *Journal of Regulatory Economics* 46.3, 261–291. DOI: [10.1007/s11149-014-9256-9](https://doi.org/10.1007/s11149-014-9256-9).
- Roberts, Michael J and Wolfram Schlenker (2013). “Identifying supply and demand elasticities of agricultural commodities: Implications for the US ethanol mandate”. *American Economic Review* 103.6, 2265–2295.
- Sheng, Jian-Xiong, Daniel J Jacob, Alexander J Turner, et al. (2018). “2010–2016 methane trends over Canada, the United States, and Mexico observed by the GOSAT satellite: contributions from different source sectors”. *Atmospheric Chemistry and Physics* 18.16, 12257–12267.
- U.S. EPA (2023). *EPA Report on the Social Cost of Greenhouse Gases: Estimates Incorporating Recent Scientific Advances*. Docket ID No. EPA-HQ-OAR-2021-0317. U.S. Environmental Protection Agency.
- (2024). “Greenhouse Gas Reporting Rule: Revisions and Confidentiality Determinations for Petroleum and Natural Gas Systems”. *Fed. Reg.* 89, 42062–42327.
- Varon, Daniel J., Daniel J. Jacob, Benjamin Hmiel, et al. (2023). “Continuous Weekly Monitoring of Methane Emissions from the Permian Basin by Inversion of TROPOMI Satellite Observations”. *Atmospheric Chemistry and Physics* 23.13, 7503–7520. DOI: [10.5194/acp-23-7503-2023](https://doi.org/10.5194/acp-23-7503-2023).